

A STELLAR PARAMETER CALIBRATION OF IUE DATA FOR THE
DETERMINATION OF THE PRESENT DAY MASS FUNCTION OF
HIGH MASS STARS

A Thesis

Submitted to the Graduate Faculty of the
Louisiana State University and
Agricultural and Mechanical College
in partial fulfillment of the
requirements for the degree of
Master of Science

in

The Department of Physics and Astronomy

by
Kenneth Thomas Taylor
B. S., Tulane University, 1984
May 2003

Computational Spectrophotometry

Dedicated to the memory of

Emery D Taylor and Ganesh Chanmugam

“There is one glory of the sun,
and another glory of the moon,
and another glory of the stars:
for one star differeth from
another star in glory.”

1 Corinthians 15:41

ACKNOWLEDGEMENTS

I would like to express my sincere appreciation and gratitude to my research advisor, Professor John S. Drilling, for his continuous help, guidance, and encouragement during this research. Appreciation also goes to Dr. Paul A. Mason for his careful review of this manuscript. In addition, I am grateful to Howard Cohl for his help with IDL software. And thanks to my mother Frances Taylor for encouragement and support. This research has made use of the Simbad database, operated at CDS, Strasbourg, France, and routines provided by the IUE Regional Data Analysis Facility (RDAF). In addition, this research has also made use of stellar atmospheres provided by Dietmar Kunze from the Universitaets-Sternwarte Muenchen and Robert Kurucz from Harvard University.

PREFACE

This thesis consists of four chapters: Chapter I serves as a general introduction to the temperatures of OB stars; Chapter II deals with the calculation of the R color index using stellar atmospheres, the R index being the ratio of the integrated de-reddened fluxes from the two International Ultraviolet Explorer (IUE) satellite cameras, and with the calculation of absolute magnitude; Chapter III deals with the calibration of R and absolute magnitude with effective temperature and surface gravity; Chapter IV derives the effective temperature, surface gravity, mass, and mass function for 156 LMC stars using IUE spectra and known apparent visual magnitudes and has the summary and conclusion.

TABLE OF CONTENTS

DEDICATION	ii
ACKNOWLEDGEMENTS	iii
PREFACE	iv
LIST OF TABLES	vii
LIST OF FIGURES	viii
ABSTACT	ix
CHAPTER	
I INTRODUCTION.....	1
1.1 Statement of the Problem	1
1.2 Background and Basic Concepts	3
1.3 Methodology of the Calibration	6
1.4 Determination of the Stellar Masses and the Initial Mass Function for Massive Stars.....	11
II DERIVING R AND ABSOLUTE MAGNITUDE FROM STELLAR ATMOSPHERES.....	13
2.1 Stellar Atmosphere Models	13
2.2 Calculation of R from the Stellar Atmosphere Models	14
2.3 Calculation of Absolute Magnitude for the Stellar Atmosphere Models	19
III THE CALIBRATION OF R AND ABSOLUTE MAGNITUDE WITH EFFECTIVE TEMPERATURE AND SURFACE GRAVITY	30
3.1 The Graphical Calibration	30
3.2 Discussion of the Calibration of R for the Model Atmospheres	34
IV THE INITIAL MASS FUNCTION FOR MASSIVE STARS IN THE LMC	35
4.1 Correcting for the Effects of Interstellar Absorption	35
4.2 Using the Stellar Temperature and Surface Gravity Calibration	36
4.3 Determining the Mass of a Star from LMC Data	37
4.4 Stellar Parameter Results.....	38
4.5 Determining Initial Mass Function for LMC	38
4.6 Conclusions	45

REFERENCES	47
APPENDIX	
A DERIVED BOLOMETRIC MAGNITUDES FOR EACH ATMOSPHERE AND FOR EACH MASS OF THE EVOLUTIONARY TRACKS	49
B IUE LOG IMAGE NUMBERS WITH STELLAR NAMES AND SPECTRAL TYPES.....	67
VITA.....	71

LIST OF TABLES

Table 1	The values of R for the Kunze (1994) atmospheres of solar metallicity	15
Table 2	The values of R for Kunze (1994) model atmospheres of varying metallicity..	16
Table 3	The values of R for the Kurucz (1979) atmospheres of solar metallicity	17
Table 4	Values of ratio R for the Kurucz (1979) atmospheres of one-third solar metallicity	18
Table 5	The V filter sensitivity function from Allen (1973).....	20
Table 6	Derived bolometric magnitude for each atmosphere and for each mass of the evolutionary tracks.....	23
Table 7	Masses in solar units used for the Kunze (1994) model atmospheres	25
Table 8	Derived absolute magnitudes for the Kunze (1994) atmospheres of solar metallicity	25
Table 9	Masses in solar units used for the Kurucz (1979) model atmospheres.....	26
Table 10	Derived absolute magnitudes for the Kurucz (1979) atmospheres of solar metallicity	27
Table 11	Absolute magnitude derived for the Kurucz (1979) atmospheres of one-third solar metallicity.....	28
Table 12	Color excess for 30 Dor stars	36
Table 13	Derived stellar parameters of LMC stars	39
Table 14	Comparison of derived stellar parameters	43
Table 15	Calculating $\log \Psi(M)$ per solar mass interval.....	44
Table 16	Number and $\log \Psi(M)$ per solar mass interval	44

LIST OF FIGURES

Figure 1: Stellar spectrum of SK -70 69 from International Ultraviolet Explorer (IUE) satellite.....	4
Figure 2: The Hertzsprung-Russell diagram for nearby stars taken from Shu (1982). The effective temperature increases towards the left and the luminosity is given as a log scale in solar units.....	5
Figure 3: The atmosphere fluxes plotted with respect to wavelength taken from Kunze's (1994) models.....	7
Figure 4: The graph of the V filter sensitivity function from Allen (1973).....	20
Figure 5: Schaerer et al's. (1993) evolutionary tracks.....	21
Figure 6: The calibration of R and magnitude differences with log g and effective temperature using the Kunze (1994) model atmospheres.....	31
Figure 7: The calibration of R and magnitude differences with log g and effective temperature using the Kurucz (1979) model atmospheres for solar metallicity.....	32
Figure 8: The calibration of R and magnitude differences with log g and effective temperature using the Kurucz (1979) model atmospheres for one-third solar metallicity.....	33
Figure 9: The initial mass function $\log \Psi(M)$ vs. $\log (M/M_{\text{sun}})$ for the LMC	45

ABSTRACT

A study of stellar atmosphere models and the photometric quantity R is presented here, with R being the ratio of the integrated de-reddened fluxes from the two wavelength regions of the International Ultraviolet Explorer (IUE) satellite cameras. The effective temperatures and surface gravities of the stellar atmospheres were calibrated against R and absolute magnitude, using stellar evolution tracks from the literature, and applied to over 156 LMC stars whose masses and mass function are then derived from the results. The results show that the effective temperatures and surface gravities of stars derived from R and absolute magnitude correlate well with those found in the literature. The slope of the initial mass function (IMF) is $\Gamma = -2.31$ for masses $85 M_{\text{sun}} \geq M \geq 15 M_{\text{sun}}$. The correlation with R and apparent magnitude could prove useful in better determining the high mass portion of the IMF.

CHAPTER I

INTRODUCTION

1.1 Statement of the Problem

An assumption of stellar evolution theory (e.g. Iben 1967) is that the initial mass of a star and the chemical composition are the primary factors in the determination of its structure and subsequent evolution. The initial mass and composition of a star, according to this theory, controls the chemical composition of the stellar material as a function of time. Ultimately, it predicts the chemical composition and amount of material ejected into the interstellar medium. Therefore, the distribution of stars as a function of mass is important in determining the chemical evolution of galaxies.

The number distribution of stars with respect to mass is called the mass function. The number of stars formed per unit volume per unit time as a function of mass is called the initial mass function or IMF. The number of stars as a function of mass right now is called the present day mass function or PDMF, and differs from the initial mass function because with time the faster evolving stars will no longer be in the present day count. If the IMF is constant over time, then it will equal the birth rate function. Stellar evolution theory shows that the more massive stars are also the hotter stars and will evolve off the main sequence faster. In addition, the initial mass function can change with time or location. For instance, as time progresses the interstellar

medium becomes richer with metals from the death of evolved stars, which in turn changes the IMF since metallicity plays a role in stellar formation and evolution.

The IMF is uncertain (Scalo 1986a), with the greatest inaccuracy occurring for the high mass stars, despite its fundamental importance and the effort of many researchers. The uncertainties at high mass are primarily because of the difficulties in determining the distances to Galactic O and B stars, due to the large amounts of obscuring dust along the line of sight to the stars. In this thesis, I develop an effective temperature and surface gravity calibration for International Ultraviolet Explorer (IUE; Boggess et al., 1978) spectra and apparent magnitude in order to determine the PDMF of high mass stars in the Large Magellanic Cloud (LMC).

The advantage of using stars in the LMC is that the distance to the LMC is reasonably well known, and the amount of interstellar reddening and absorption for the LMC is significantly less than that for galactic high mass stars. The amount of reddening for the stars in the sample is important because we need to determine the absolute magnitudes, effective temperatures, and bolometric corrections for these stars. All three of these quantities are reddening dependent; hence, the uncertainties will be much smaller in the LMC as compared to galactic OB associations. These observationally determined quantities are compared to theoretical evolutionary tracks to determine the PDMF of high mass stars. In addition, we may consider that all of the stars in the LMC are at approximately the same distance. If a collection of stars is reasonably thought to have been formed at the same time, then the PDMF is equal to the IMF for all stars with lifetimes greater than the age of the cluster or association. For this reason, Massey et al. (1989 a,b) and Hill et al. (1994 a,b,c) studied stellar populations of young clusters and OB associations in the LMC. However, since

massive stars are rare in any one OB association we would not be able to obtain a statistically significant result due to the paucity of massive stars. Therefore, to determine the IMF for massive stars a much larger sample is useful, such as that used by Humphreys and McElroy (1984) who used all spectral types of massive stars available in the literature.

In this thesis, we will attempt to determine the mass of a star from the surface gravity ($\log g$), effective temperature (T_{eff}), and luminosity (L) of the star. The effective temperature of a star is the temperature a black body would have to have in order for it to produce the surface flux as observed. The luminosity is determined from the absolute bolometric magnitude (M_{bol}). The absolute bolometric magnitude is determined from the bolometric correction (B.C.), the known distance, and apparent visual magnitude. The effective temperature and surface gravity may be determined from ultraviolet spectra data and absolute magnitude using the calibration derived in this thesis, as we will show.

1.2 Background and Basic Concepts

Most of the information available from stars is in the form of electromagnetic radiation. Physical processes determine how the light or electromagnetic radiation is emitted as a function of wavelength or frequency. So stars have what electrical engineers would call a frequency response, that is, output with respect to frequency. However, astronomers look at the flux of light versus its wavelength and call it the spectrum of a star. An example of a stellar spectrum used in this thesis is shown in Figure 1 and was obtained from the IUE archive. The luminosity of a star is a measure of its power output or energy per unit time, ergs/sec. The flux is the energy per unit time per unit surface area per unit wavelength, $\text{ergs sec}^{-1} \text{cm}^{-2} \text{\AA}^{-1}$.

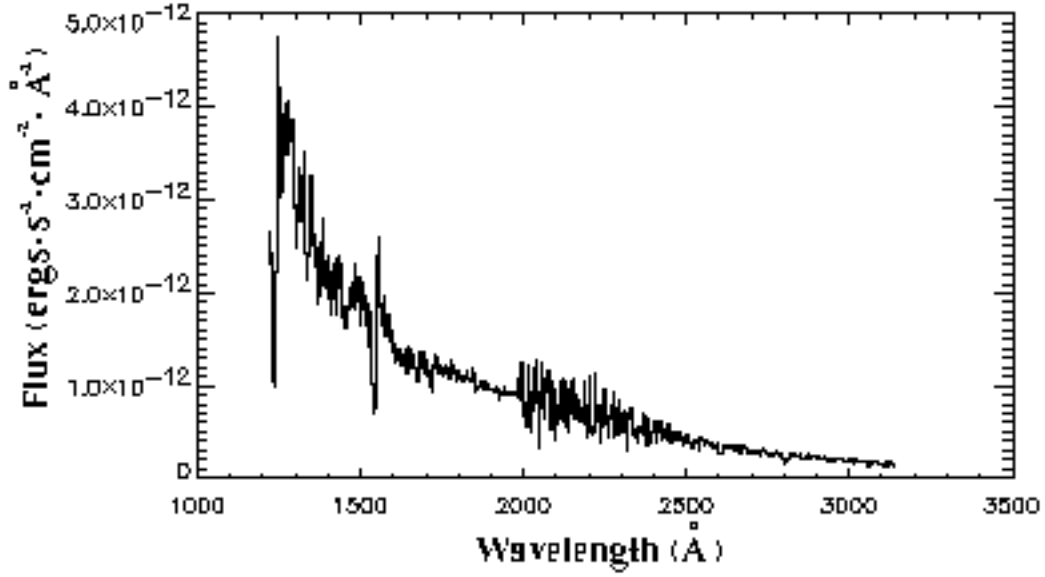


Figure 1: Stellar spectrum of SK -70 69 from International Ultraviolet Explorer (IUE) satellite.

A powerful tool for the study of stellar evolution and the evolution of stellar populations is the Hertzsprung-Russell (H-R) diagram. The H-R diagram is a plot of the luminosities (or absolute magnitudes) of stars against their effective temperatures. An example of an H-R diagram is shown in Figure 2. The particular stars that are hotter than 25,000 K on the H-R diagram motivate the direction of this thesis because of the uncertainty of the mass function for high mass stars.

An H-R diagram of this form is most meaningful for a sample of stars at a common distance. This is because uncertainties in the distances to individual stars will blur the H-R diagram, since the observational quantity being measured is apparent magnitude, m_V , which is related to absolute magnitude, M_V , and the distance, d , by

$$m_V - M_V = 5 \log (d/10\text{pc}). \quad (1)$$

The absolute bolometric magnitude is a measure of the total light emitted from the star at all wavelengths and is related to the absolute visual magnitude via

$$M_{\text{bol}} = M_V + \text{B.C.}, \quad (2)$$

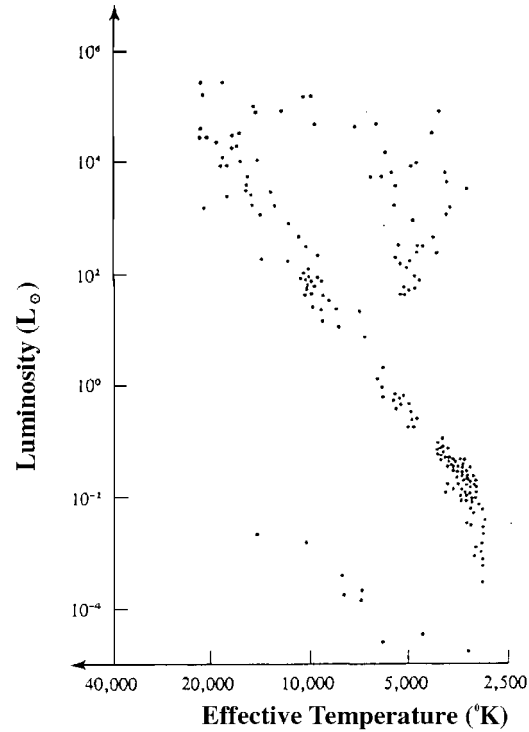


Figure 2: The Hertzsprung-Russell diagram for nearby stars taken from Shu (1982). The effective temperature increases towards the left and the luminosity is given as a log scale in solar units.

where B.C. is known as the bolometric correction. We can derive the star's luminosity in terms of the solar luminosity, given the known bolometric luminosity of the sun, through the equation

$$M_{\text{bol}_1} - M_{\text{bol}_2} = 2.5 \log (L_2 / L_1). \quad (3)$$

Therefore, if the apparent magnitudes of a sample of stars, all at a known distance, and their bolometric corrections are measured, then we may derive the luminosities of the stars using equations 1-3. Mass can be found with the additional information about effective temperature and $\log g$ (for stars of a given chemical composition).

1.3 Methodology of the Calibration

We must also determine the effective temperatures of the stars in the sample. High mass stars have their greatest output of energy in the ultraviolet part of the spectrum. Therefore, in this thesis we examine a method using ultraviolet observations and model atmosphere spectra. In Figure 3 one can see the flux plotted against wavelength for one set of 24 model atmospheres used in this project. Note that the spectra look similar. The hotter stars have curves that are shifted towards shorter wavelengths, which is similar to Wien's displacement law for thermal radiation: "if the temperature T increases, there are more photons with shorter wavelengths (higher energy). In particular, the wavelength of maximum emission, λ_{\max} , shifts with changing temperature according to the law $\lambda_{\max} T = 0.29 \text{ cm K}$ " (Shu 1982). Wien's law follows from Planck's law:

$$E(\lambda, T) = 2hc^2 \lambda^{-5} / (e^{hc/\lambda kT} - 1). \quad (4)$$

A model continuous spectrum is a weighted average of the Planck curve, and it is the solution for the equation of transfer of a stellar atmosphere. In Figure 3 the lines in the curve represent absorption lines in the atmosphere. The absorption lines are caused by atomic transitions in the stellar atmosphere. Shortward of the Balmer jump large amounts of absorption are due to the ionization of atomic hydrogen.

The effective temperature of a star is the temperature a black body would have to have in order for it to produce the same surface flux. From observations, there are three common ways to find the effective temperature of a star. The first method is the use of the luminosity of the star. The luminosity is the total energy emitted per second

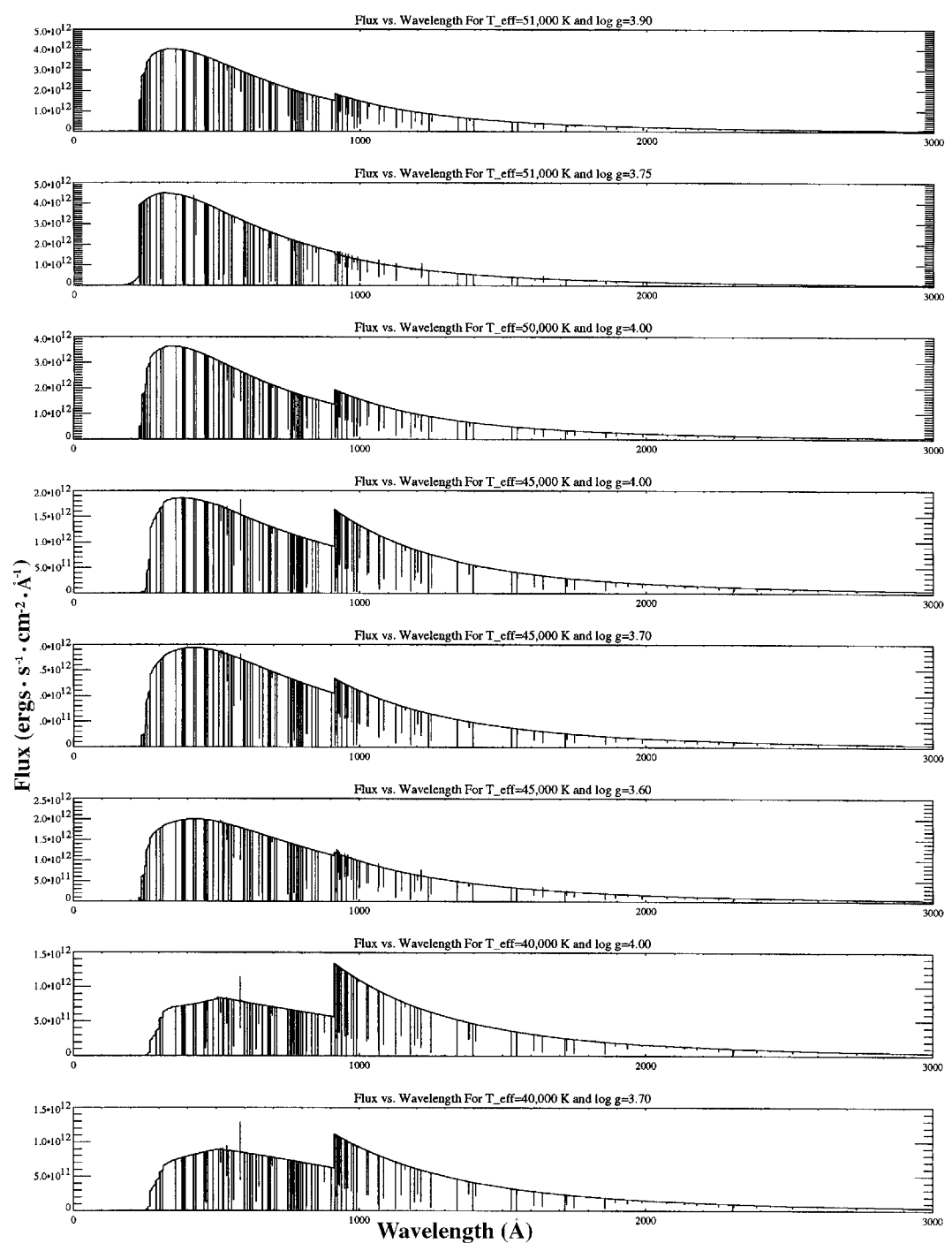


Figure 3: The atmosphere fluxes plotted with respect to wavelength taken from Kunze's (1994) models.

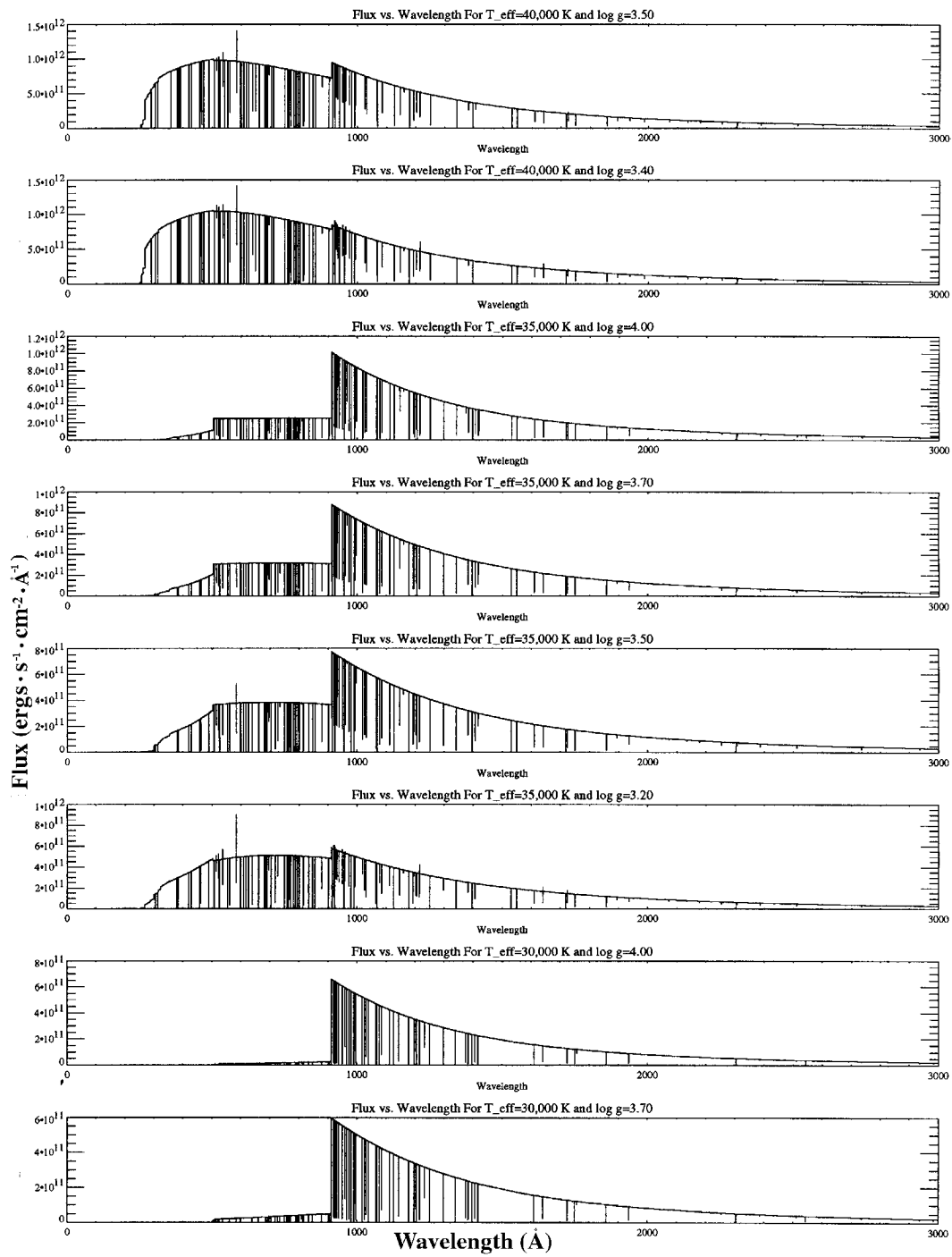


Figure 3b: Continuation of Figure 3

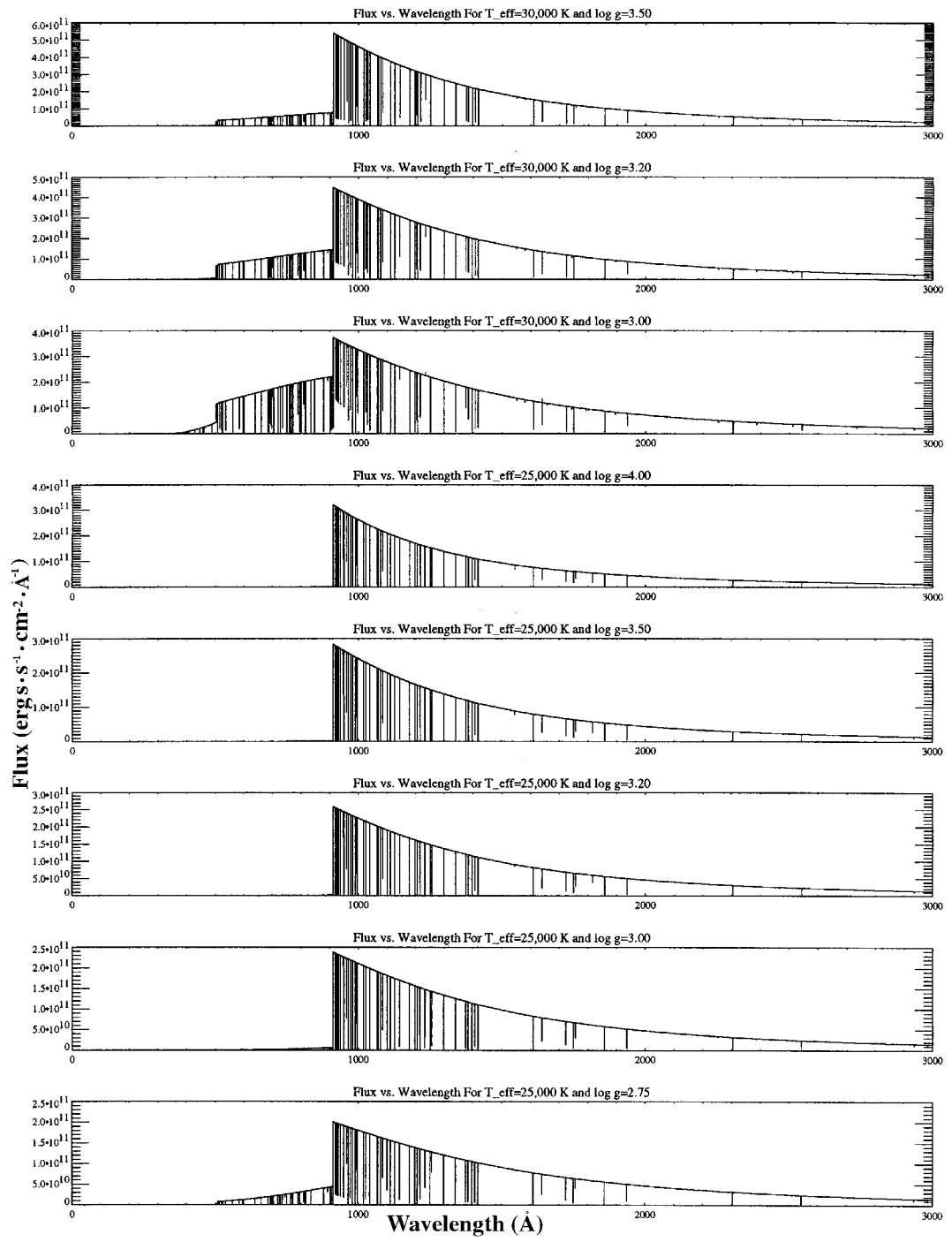


Figure 3c: Continuation of Figure 3

and is related to the effective temperature. If the luminosity and the radius of the star are known, then the effective temperature can be found from the definition of effective temperature:

$$L = 4\pi\mathcal{R}^2\sigma T^4, \quad (5)$$

where σ is the Stefan-Boltzman constant and \mathcal{R} is the radius of the star. The radius can be found from the angular diameter of the star if its distance is known. However, angular diameters can only be measured for a couple of dozen stars. The second method is to use the relative strengths of the spectral lines since they are temperature dependent. The third method is called the color temperature, and it uses two wide band filters to determine the ratio of intensities in those ranges of the electromagnetic spectrum. This requires a calibration of the ratio to the temperature, which is what this thesis is attempting to do.

The IUE satellite is well suited for studying spectra of young high mass stars. This is because young high mass stars have their peak brightness in the ultraviolet part of the spectrum. For this reason, we studied the ratio of the integrated de-reddened fluxes for the two IUE satellite cameras. This ratio we define as

$$R = \int_{1200}^{1945} F_{\lambda} d\lambda \bigg/ \int_{1945}^{3120} F_{\lambda} d\lambda, \quad (6)$$

with F_{λ} being the de-reddened flux per unit wavelength.

The purpose of this thesis is to show that the effective temperature and the surface gravity of a star are strongly correlated with R and absolute magnitude. In order to show this correlation, stellar atmosphere models were obtained from Dietmar Kunze (1994) of the Universitaets-Sternwarte Muenchen and Robert Kurucz (1979) of Harvard

University. The model atmospheres vary in effective temperature, surface gravity, and metallicity. Therefore, by determining the values of R and absolute magnitude for each of the stellar atmospheres (using evolutionary tracks) we plan to show, with use of graphs, the correlation to the effective temperature and surface gravity for stars with similar metallicity (see Figures 6-8).

1.4 Determination of the Stellar Masses and the Initial Mass Function for Massive Stars

According to the theory of stellar atmospheres, the spectrum of a star is a function of effective temperature, surface gravity, and metallicity:

$$F_{\lambda} = f(T_{\text{eff}}, g, Z). \quad (7)$$

The bolometric correction is 2.5 times the log of the total flux divided by the visual flux:

$$\text{B.C.} = 2.5 \log \frac{\int F_{\lambda} d\lambda}{\int F_{\lambda} V_{\lambda} d\lambda} + \text{Const.} \quad (8)$$

The sensitivity function, V_{λ} , is the fraction of light as a function of wavelength in the visual wavelength range that passes through a standard V filter. Equation 8 and stellar atmosphere models show that bolometric correction can be expressed as a function of effective temperature, surface gravity, and metallicity:

$$\text{B.C.} = f(T_{\text{eff}}, g, Z). \quad (9)$$

Stellar atmosphere models show that R (see equation 6) can be expressed as a function of effective temperature, surface gravity, and metallicity:

$$R = f(T_{\text{eff}}, g, Z). \quad (10)$$

In the next chapter, we see that bolometric magnitude can be expressed as a function of effective temperature and mass, \mathcal{M} , using evolutionary tracks for hot massive stars:

$$M_{\text{bol}} = f(T_{\text{eff}}, \mathcal{M}). \quad (11)$$

A star's surface gravity is defined as

$$g = G \mathcal{M} / \mathcal{R}^2, \quad (12)$$

where G is the gravitational constant. From the definition of effective temperature, the luminosity is

$$L_* = 4\pi \mathcal{R}^2 \sigma T_{\text{eff}}^4. \quad (13)$$

Bolometric magnitude is related to luminosity by

$$M_{\text{bol}*} - M_{\text{bol}\text{sun}} = -2.5 \log(L_* / L_{\text{sun}}), \quad (14)$$

with

$$M_{\text{bol}} = M_V + \text{B.C.} \quad (15)$$

We now have seven equations (9-15) with unknowns \mathcal{M} , g , T_{eff} , B.C., \mathcal{R} , L , M_{bol} , for stars of a given chemical composition if R and M_V are known.

As was discussed briefly in the last section, the goal of this thesis is to show that you can compare the R and M_V of a star to stellar atmospheres and evolutionary tracks, thereby, finding the star's effective temperature, surface gravity, and ultimately, mass. With this (and proper correction for the incompleteness of the sample) we may determine the IMF for high mass stars in objects like the LMC. The LMC is a good choice for a project like this because its distance is reasonably well known, and hence you can determine the absolute magnitude for a star from its apparent magnitude (see equation 1). A better understanding of the IMF for high mass stars is important for the (future) study of galactic evolution.

CHAPTER II

DERIVING R AND ABSOLUTE MAGNITUDE FROM STELLAR ATMOSPHERES

In this chapter, the determination of R for two sets of stellar atmosphere models is presented. Using evolutionary tracks, absolute magnitudes are derived for each atmosphere with results presented in this chapter as well. In Chapter 3 a calibration of surface gravity and effective temperature is made by plotting the atmospheres in the R vs. absolute magnitude plane, and in Chapter 4 this calibration is used to derive the mass of 156 LMC stars.

2.1 Stellar Atmosphere Models

To calculate a stellar atmosphere the atmospheric composition, effective temperature, and surface gravity of the star must be given. The populations of various energy levels of the elements that make up the chemical composition are affected by the use or non-use of the assumption of local thermodynamic equilibrium (LTE; Collins 1989), which is that the particles of the gas in a small volume can be characterized by a single temperature along the mean free path of a photon. Deep inside a star the mean free path of photons is small, so the assumption of LTE is reasonable. However, near the surface of a star enough photons escape so that LTE is no longer valid. The spectral lines of atmospheres calculated from LTE models are weaker than those of observed high temperature stars with the same surface gravity (Mihalas 1978).

2.2 Calculation of R from the Stellar Atmosphere Models

The stellar atmospheres used were the non-LTE model atmospheres for hot stars computed by Dietmar Kunze (1994) from the Universitaets-Sternwarte Muenchen, and the LTE model atmospheres of Robert Kurucz (1979) from Harvard University. The elements that make up the chemical composition used in the determination of the Kunze models include H, He, C, N, O, Si, Ar, Mg, Al, and Na. Kunze assumed plane-parallel geometry (no curvature), hydrostatic stratification (no mass loss), and radiative equilibrium (no convection). The Kunze model atmospheres ranged over 7 different effective temperatures, T_{eff} , from 25,000 K to 51,000 K, and 10 different surface gravities, $\log g$, from 4.0 down to the Eddington limit (the point where the outward radiative acceleration equals the inward acceleration of gravity).

The data from the Kunze models were given as a table of Eddington fluxes per unit frequency as a function of wavelength (ergs/s/cm²/Hz). Since $f_{\lambda} d\lambda = f_{\nu} d\nu$ and $c = \nu\lambda$, then $d\nu = -c / \lambda^2 d\lambda$, and therefore

$$f_{\nu} d\nu = f_{\nu} (-c/\lambda^2) d\lambda = f_{\lambda} d\lambda. \quad (16)$$

The quantity $(-c/\lambda^2)$ can be multiplied by each Eddington flux per frequency interval (f_{ν}) to obtain the Eddington flux per unit wavelength (ergs/s/cm²/Å). R is derived by numerically integrating the flux over an interval of wavelength from the equation

$$R = \int_{1200}^{1945} F_{\lambda} d\lambda / \int_{1945}^{3120} F_{\lambda} d\lambda, \quad (17)$$

with the results from the Kunze atmospheres of solar metallicity given in Table 1.

Table 1 Values of R for the Kunze (1994) atmospheres of solar metallicity

T_{eff} (K)	log g (cgs)									
	4.00	3.90	3.75	3.70	3.60	3.50	3.40	3.20	3.00	2.75
25000	2.247	-	-	-	-	2.175	-	2.094	2.008	1.877
30000	2.446	-	-	2.354	-	2.277	-	2.140	2.029	-
35000	2.445	-	-	2.344	-	2.269	-	2.132	-	-
40000	2.473	-	-	2.379	-	2.300	2.252	-	-	-
45000	2.524	-	-	2.418	2.367	-	-	-	-	-
50000	2.568	-	-	-	-	-	-	-	-	-
51000	-	2.531	2.437	-	-	-	-	-	-	-

In Table 1 we note that in the $\log g = 4.00$ column, when you go down the table, or increase temperature, R increases from around 2.2 to 2.5. Looking at the effective temperature equals 25,000 K row, going right across the table, or decreasing $\log g$, R decreases from around 2.25 to 1.88. In Table 2 we show R for the Kunze atmospheres for varying metallicity. One will notice that for a given T_{eff} and $\log g$, the value of R changes very little by increasing metallicity. In Table 1 we clearly see that the change in R versus T_{eff} or $\log g$ is greater than against metallicity in Table 2.

In order to make use of the IUE data for the LMC OB stars with R values below two, atmospheres are needed for smaller temperatures than those provided by Kunze. The 218 LTE model atmospheres with solar metallicity obtained from Robert Kurucz (1979) range from 5,000 K to 50,000 K and yield the R results in Table 3. Unlike the Kunze models, R is somewhat affected by metallicity for the Kurucz atmospheres. The metallicity of the LMC is around 0.4 solar (Schaerer et al. 1993). Later on, we will use the Kurucz atmospheres of one-third solar metallicity (Table 4; which should be close enough to 0.4), and for future reference we also derive R for atmospheres of solar metallicity.

Table 2 The values of R for Kunze (1994) model atmospheres with varying metallicity

T_{eff} (K)	log g (cgs)	Solar Metallicity					
		0.01	0.1	0.3	1.0	3.0	10.0
51000	3.90	2.53	2.53	2.53	2.53	2.54	2.56
51000	3.75	2.46	2.43	2.43	2.44	2.45	2.48
50000	4.00	2.57	2.57	2.57	2.57	2.57	2.58
45000	4.00	2.52	2.52	2.52	2.52	2.53	2.53
45000	3.70	2.41	2.41	2.42	2.42	2.42	2.44
45000	3.60	2.40	2.36	2.37	2.36	2.36	2.36
40000	4.00	2.47	2.47	2.47	2.47	2.47	2.47
40000	3.70	2.39	2.38	2.38	2.38	2.38	2.38
40000	3.50	2.32	2.31	2.30	2.30	2.30	2.30
40000	3.40	2.28	2.26	2.25	2.25	2.25	2.25
35000	4.00	2.44	2.45	2.45	2.44	2.44	2.43
35000	3.70	2.35	2.35	2.34	2.34	2.34	2.34
35000	3.50	2.28	2.27	2.27	2.26	2.27	2.26
35000	3.20	2.15	2.14	2.13	2.13	2.13	2.13
30000	4.00	2.44	2.44	2.45	2.45	2.45	2.45
30000	3.70	2.35	2.35	2.35	2.36	2.36	2.36
30000	3.50	2.28	2.28	2.28	2.28	2.28	2.28
30000	3.20	2.16	2.14	2.14	2.14	2.14	2.13
30000	3.00	2.05	2.03	2.03	2.02	2.02	2.02
25000	4.00	2.27	2.25	2.25	2.25	2.25	2.25
25000	3.50	2.20	2.18	2.18	2.17	2.17	2.17
25000	3.20	2.12	2.10	2.09	2.09	2.09	2.09
25000	3.00	2.03	2.02	2.01	2.01	2.01	2.01
25000	2.75	1.90	1.88	1.88	1.87	1.88	1.88

In Table 3 values of R as a function of T_{eff} and $\log g$ for Kurucz atmospheres of solar metallicity are presented, and in Table 4 values of R as a function of T_{eff} and $\log g$ for Kurucz atmospheres of one-third solar metallicity are shown. In both Tables 3 and 4 we notice that R increases if $\log g$ is constant and T_{eff} increases.

2.3 Calculation of Absolute Magnitude for the Stellar Atmosphere Models

The absolute magnitude of each atmosphere is found through use of the equation

$$M_{V_1} - M_{V_2} = -2.5 \log \frac{4\pi R_1^2 \int_0^\infty F_\lambda^{(1)} V_\lambda d\lambda}{4\pi R_2^2 \int_0^\infty F_\lambda^{(2)} V_\lambda d\lambda}, \quad (18)$$

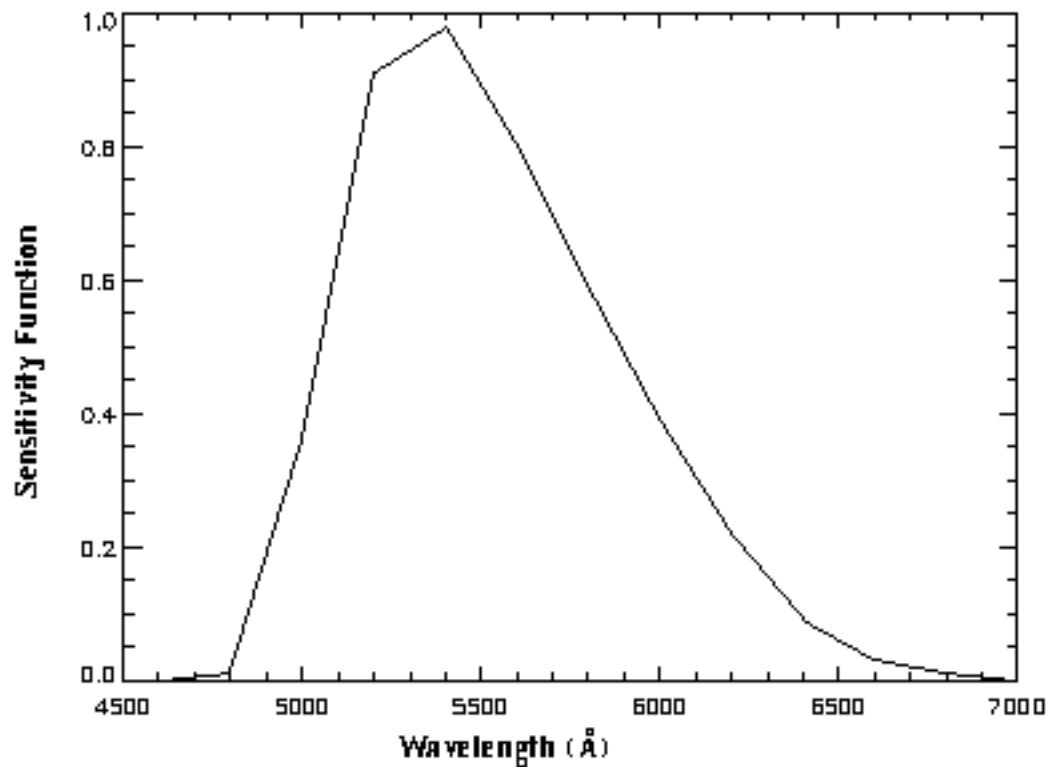
with an atmosphere of the sun for the second model. Equation 18 requires knowing radius \mathcal{R} for each model. However, \mathcal{R} is eliminated because $g = G M / \mathcal{R}^2$, so that

$$M_{V_1} = -2.5 \log \frac{4\pi M_1 g_2 \int_0^\infty F_\lambda^{(1)} V_\lambda d\lambda}{4\pi M_2 g_1 \int_0^\infty F_\lambda^{(2)} V_\lambda d\lambda} + M_{V_2}, \quad (19)$$

with g , and F_λ given by the data from the models. V_λ is called the sensitivity function and is the fraction of light in the visual wavelength range that passes through a standard V filter as a function of wavelength. In this project we used the V filter sensitivity function found in Allen (1973), which is given in Table 5 and plotted in Figure 4. We adopt the absolute magnitude of the sun to be 4.82 with the surface gravity being 27,400 cm/s^2 , Allen (2000). We determine the visual flux of a solar atmosphere from Kurucz (1979) to be $5.97 \times 10^8 \text{ ergs/s/cm}^2$, using the sensitivity function. In order to find the

Table 5 The V filter sensitivity function from Allen (1973)

Wavelength (Ångstroms)	Filter Percentage
4600	0.00
4800	0.01
5000	0.36
5200	0.91
5400	0.98
5600	0.80
5800	0.59
6000	0.39
6200	0.22
6400	0.09
6600	0.03
6800	0.01
7000	0.00

**Figure 4:** The graph of the V filter sensitivity function from Allen (1973) .

absolute magnitude for each atmosphere, the mass is the only parameter not known to us at this point.

From equation 19 we can find the absolute magnitude of each atmosphere once we derive a mass for each atmosphere. For this purpose, we will use Schaerer et al's. (1993) evolutionary tracks, taken from Walborn et al. (1995), for massive stars evolving off the main sequence (see Figure 5).

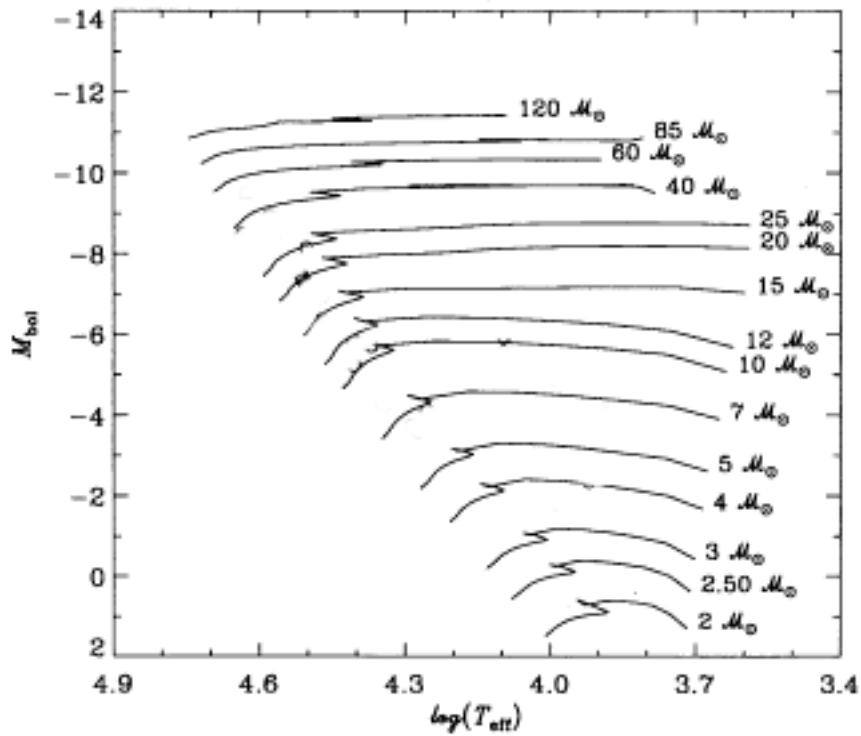


Figure 5: Schaerer et al's. (1993) evolutionary tracks.

In order to find a mass for each atmosphere using the Schaerer et al. evolutionary tracks, we derive the following relations starting with the definition of bolometric magnitude:

$$M_{\text{bol}_1} - M_{\text{bol}_2} = 2.5 \log (L_2 / L_1). \quad (20)$$

Using the sun for M_{bol_2} and L_2 gives

$$M_{\text{bol}_1} = M_{\text{bol}_{\text{sun}}} + 2.5 \log L_{\text{sun}} - 2.5 \log L_1, \quad (21)$$

and from Allen (2000) we adopt $M_{\text{bol}_{\text{sun}}} = 4.74$ and $L_{\text{sun}} = 3.845 \times 10^{33}$ which simplifies the equation to

$$M_{\text{bol}_1} = 88.702 - 2.5 \log L_1. \quad (22)$$

Because $L = 4\pi \mathcal{R}^2 \sigma T_{\text{eff}}^4$ and $g = G\mathcal{M} / \mathcal{R}^2$, then $L = 4\pi G\mathcal{M} \sigma T_{\text{eff}}^4 / g$. After inserting the values for the constants we find that

$$L = 9.4574 \times 10^{22} \mathcal{M}_{\text{solar}} T_{\text{eff}}^4 / g, \quad (23)$$

where $\mathcal{M}_{\text{solar}}$ is in units of solar mass and everything else is cgs units. Therefore, the bolometric magnitude for an atmosphere is

$$M_{\text{bol}_1} = 88.702 - 2.5 \log (9.4574 \times 10^{22} \mathcal{M}_{\text{solar}} T_{\text{eff}}^4 / g). \quad (24)$$

Equation 24 shows that bolometric magnitude is a function of mass, effective temperature, and surface gravity. Evolutionary tracks in Figure 5 show that bolometric magnitude is a function of mass and effective temperature:

$$M_{\text{bol}_1} = f(\mathcal{M}, T_{\text{eff}}). \quad (25)$$

Each atmosphere specifies an effective temperature and surface gravity, so we have two equations with the two unknowns of mass and bolometric magnitude. One has to choose the one mass for a given atmosphere that satisfies the corresponding evolutionary track of Figure 5. For each atmosphere, the bolometric magnitudes for each mass are shown in Table 6, and the resulting masses are given in Table 7.

Table 6 Derived bolometric magnitudes for each atmosphere and for each mass of the evolutionary tracks

Solar Mass	T_{eff} (K) log g	51,000 3.90	51,000 3.75	50,000 4.00	45,000 4.00	45,000 3.70	45,000 3.60
120		-11.26	-11.64	-10.93	-10.47	-11.22	-11.47
85		-10.89	-11.26	-10.55	-10.09	-10.84	-11.09
60		-10.51	-10.88	-10.17	-9.71	-10.46	-10.71
40		-10.07	-10.44	-9.73	-9.27	-10.02	-10.27
25		-9.56	-9.93	-9.22	-8.76	-9.51	-9.76
20		-9.32	-9.69	-8.98	-8.52	-9.27	-9.52
15		-9.00	-9.38	-8.67	-8.21	-8.96	-9.21
12		-8.76	-9.14	-8.43	-7.97	-8.72	-8.97
10		-8.56	-8.94	-8.23	-7.77	-8.52	-8.77
7		-8.18	-8.55	-7.84	-7.38	-8.13	-8.38
5		-7.81	-8.19	-7.47	-7.02	-7.77	-8.02
4		-7.57	-7.94	-7.23	-6.77	-7.52	-7.77
3		-7.26	-7.63	-6.92	-6.46	-7.21	-7.46
2.5		-7.06	-7.43	-6.72	-6.26	-7.01	-7.26
2		-6.82	-7.19	-6.48	-6.02	-6.77	-7.02
Solar Mass	T_{eff} (K) log g	40,000 4.00	40,000 3.70	40,000 3.50	40,000 3.40	35,000 4.00	35,000 3.70
120		-9.96	-10.71	-11.21	-11.46	-9.38	-10.13
85		-9.58	-10.33	-10.83	-11.08	-9.00	-9.75
60		-9.20	-9.95	-10.45	-10.70	-8.62	-9.37
40		-8.76	-9.51	-10.01	-10.26	-8.18	-8.93
25		-8.25	-9.00	-9.50	-9.75	-7.67	-8.42
20		-8.01	-8.76	-9.26	-9.51	-7.43	-8.18
15		-7.70	-8.45	-8.95	-9.20	-7.12	-7.87
12		-7.46	-8.21	-8.71	-8.96	-6.88	-7.63
10		-7.26	-8.01	-8.51	-8.76	-6.68	-7.43
7		-6.87	-7.62	-8.12	-8.37	-6.29	-7.04
5		-6.51	-7.26	-7.76	-8.01	-5.93	-6.68
4		-6.26	-7.01	-7.51	-7.76	-5.68	-6.43
3		-5.95	-6.70	-7.20	-7.45	-5.37	-6.12
2.5		-5.75	-6.50	-7.00	-7.25	-5.17	-5.92
2		-5.51	-6.26	-6.76	-7.01	-4.93	-5.68

Table 6b Continuation of Table 6

Solar Mass	T_{eff} (K) log g	35,000 3.50	35,000 3.20	30,000 4.00	30,000 3.70	30,000 3.50	30,000 3.20
120		-10.63	-11.38	-8.71	-9.46	-9.96	-10.71
85		-10.25	-11.00	-8.33	-9.08	-9.58	-10.33
60		-9.87	-10.62	-7.95	-8.70	-9.20	-9.95
40		-9.43	-10.18	-7.51	-8.26	-8.76	-9.51
25		-8.92	-9.67	-7.00	-7.75	-8.25	-9.00
20		-8.68	-9.43	-6.76	-7.51	-8.01	-8.76
15		-8.37	-9.12	-6.45	-7.20	-7.70	-8.45
12		-8.13	-8.88	-6.21	-6.96	-7.46	-8.21
10		-7.93	-8.68	-6.01	-6.76	-7.26	-8.01
7		-7.54	-8.29	-5.62	-6.37	-6.87	-7.62
5		-7.18	-7.93	-5.26	-6.01	-6.51	-7.26
4		-6.93	-7.68	-5.01	-5.76	-6.26	-7.01
3		-6.62	-7.37	-4.70	-5.45	-5.95	-6.70
2.5		-6.42	-7.17	-4.50	-5.25	-5.75	-6.50
2		-6.18	-6.93	-4.26	-5.01	-5.51	-6.26

Solar Mass	T_{eff} (K) log g	30,000 3.00	25,000 4.00	25,000 3.50	25,000 3.20	25,000 3.00	25,000 2.75
120		-11.21	-7.91	-9.16	-9.91	-10.41	-11.04
85		-10.83	-7.54	-8.79	-9.54	-10.04	-10.67
60		-10.45	-7.16	-8.41	-9.16	-9.66	-10.29
40		-10.01	-6.72	-7.97	-8.72	-9.22	-9.85
25		-9.50	-6.21	-7.46	-8.21	-8.71	-9.34
20		-9.26	-5.97	-7.22	-7.97	-8.47	-9.09
15		-8.95	-5.66	-6.91	-7.66	-8.16	-8.78
12		-8.71	-5.41	-6.66	-7.41	-7.91	-8.54
10		-8.51	-5.22	-6.47	-7.22	-7.72	-8.34
7		-8.12	-4.83	-6.08	-6.83	-7.33	-7.95
5		-7.76	-4.46	-5.71	-6.46	-6.96	-7.59
4		-7.51	-4.22	-5.47	-6.22	-6.72	-7.35
3		-7.20	-3.91	-5.16	-5.91	-6.41	-7.03
2.5		-7.00	-3.71	-4.96	-5.71	-6.21	-6.84
2		-6.76	-3.47	-4.72	-5.47	-5.97	-6.59

Table 7 Masses in solar units used for the Kunze (1994) model atmospheres

T_{eff} (K)	log g (cgs)									
	4.00	3.90	3.75	3.70	3.60	3.50	3.40	3.20	3.00	2.75
25000	10	-	-	-	-	12	-	20	25	60
30000	12	-	-	20	-	23	-	40	73	-
35000	25	-	-	33	-	40	-	120	-	-
40000	40	-	-	60	-	103	120	-	-	-
45000	60	-	-	103	120	-	-	-	-	-
50000	85	-	-	-	-	-	-	-	-	-
51000	-	120	120	-	-	-	-	-	-	-

Table 8 Derived absolute magnitudes for the Kunze (1994) atmospheres of solar metallicity

T_{eff} (K)	log g (cgs)									
	4.00	3.90	3.75	3.70	3.60	3.50	3.40	3.20	3.00	2.75
25000	-2.536	-	-	-	-	-4.009	-	-5.341	-6.108	-7.677
30000	-3.129	-	-	-4.457	-	-5.114	-	-6.455	-7.580	-
35000	-4.254	-	-	-5.303	-	-6.001	-	-7.863	-	-
40000	-4.969	-	-	-6.272	-	-7.164	-7.541	-	-	-
45000	-5.530	-	-	-6.825	-7.209	-	-	-	-	-
50000	-6.025	-	-	-	-	-	-	-	-	-
51000	-	-6.653	-6.987	-	-	-	-	-	-	-

In Table 7 we note that the masses derived are larger if T_{eff} is constant and log g decreases, or log g is constant and T_{eff} increases. From the masses given in Table 7, we can now derive absolute magnitudes from equation 19 for the Kunze atmospheres of solar metallicity with results shown in Table 8. In Table 8 we note that absolute magnitudes decreases if effective temperature is constant and log g decreases, or log g is constant and T_{eff} increases. We now turn to Kurucz model atmospheres and apply the same process with the results given in Tables 9-11.

Appendix A gives the bolometric magnitudes for the 15 different masses from the evolutionary tracks from Schaerer et al. for each of the 218 Kurucz model atmospheres. Using the same method we used for the Kunze atmospheres, masses were chosen using evolutionary tracks for each of the 218 Kurucz models and are presented in Table 9. As before, absolute magnitudes can be derived for the Kurucz atmospheres from equation 19 with results shown in Table 10 for the atmospheres of solar metallicity. Table 11 shows the absolute magnitudes for the atmospheres of one-third solar metallicity.

In Table 9 the masses derived increase if T_{eff} is constant and $\log g$ decreases, or $\log g$ is constant and T_{eff} increases. In both Tables 10 and 11 absolute magnitude decreases if effective temperature is constant and $\log g$ decreases, or $\log g$ is constant and T_{eff} increases. The difference in absolute magnitude between Tables 10 and 11 is seen to be small, but not as small as for the Kunze atmospheres. In Chapter 3 we will show that if one measures R for a star and calculates the absolute magnitude from its apparent magnitude and distance, then T_{eff} and $\log g$ can be found graphically.

CHAPTER III

THE CALIBRATION OF R AND ABSOLUTE MAGNITUDE WITH EFFECTIVE TEMPERATURE AND SURFACE GRAVITY

If you observe a star, measure R , and calculate absolute magnitude from its apparent magnitude and distance, you can then graphically find its effective temperature and surface gravity from one of the figures presented in this chapter. That is, assuming that the star lies on one of the Schaerer et al. evolutionary tracks. In Chapter 4 we will find effective temperatures and surface gravities of LMC stars from these figures.

3.1 The Graphical Calibration

Table 1 gives the results of R as a function of T_{eff} and $\log g$ for the Kunze atmospheres for solar metallicity. Table 8 gives the results for absolute magnitudes. Figure 6 graphically shows how R and absolute magnitude vary with T_{eff} and $\log g$ for these atmospheres. In Figure 6, moving to the left for decreasing absolute magnitude, the atmospheres with the same T_{eff} move to the left and downwards. The atmospheres with the same $\log g$ move to the left and upwards when absolute magnitude decreases.

A star's ultraviolet spectrum gives its R , and from its apparent magnitude and distance the absolute magnitude can be derived, with a correction for absorption. To find the T_{eff} and $\log g$ from R and absolute magnitude one uses Figure 6. You simply plot a star's R and absolute magnitude in Figure 6, and then interpolate to find the T_{eff} and $\log g$.

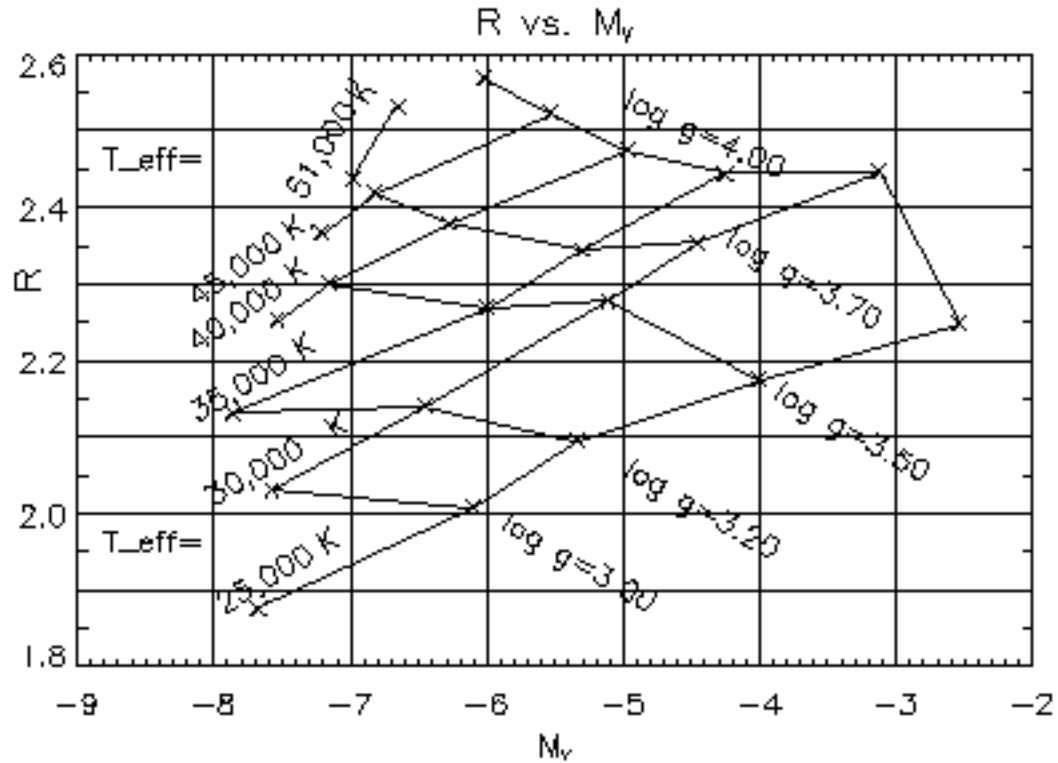


Figure 6: The calibration of R and absolute magnitude with $\log g$ and effective temperature using the Kunze (1994) model atmospheres.

Unfortunately, only stars with R values over 1.8 can be plotted in Figure 6, and in our sample of LMC stars most are below this value. For this reason, we turned to the LTE Kurucz atmospheres and applied the same process as before. Tables 3-4 show the R of the Kurucz atmospheres of one solar metallicity and one-third solar metallicity respectively. Tables 10-11 show the absolute magnitudes of the Kurucz atmospheres of solar metallicity and one-third solar metallicity respectively. Figure 7 graphically shows how R and absolute magnitude vary with T_{eff} and $\log g$ for Kurucz atmospheres of one solar metallicity. Figure 8 does the same for one-third solar metallicity.

As in Figure 6, moving to the left in Figures 7 and 8 for decreasing absolute magnitude, the atmospheres with the same T_{eff} move to the left and downwards (over

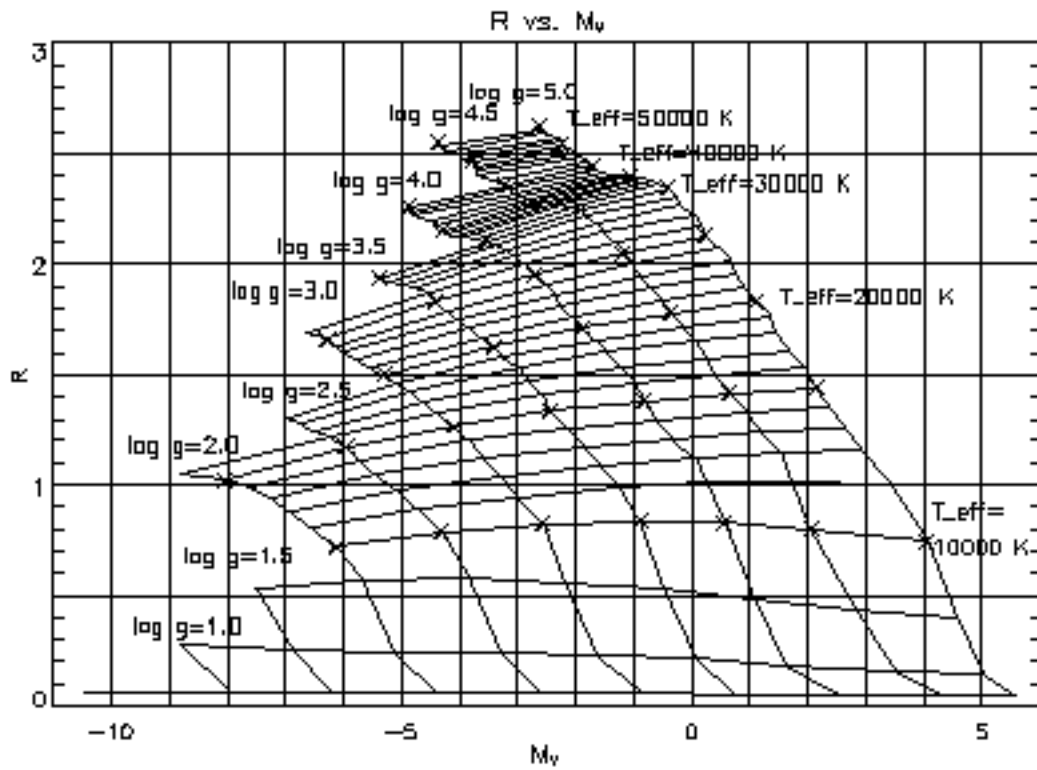


Figure 7: The calibration of R and absolute magnitude with $\log g$ and effective temperature using the Kurucz (1979) model atmospheres for solar metallicity.

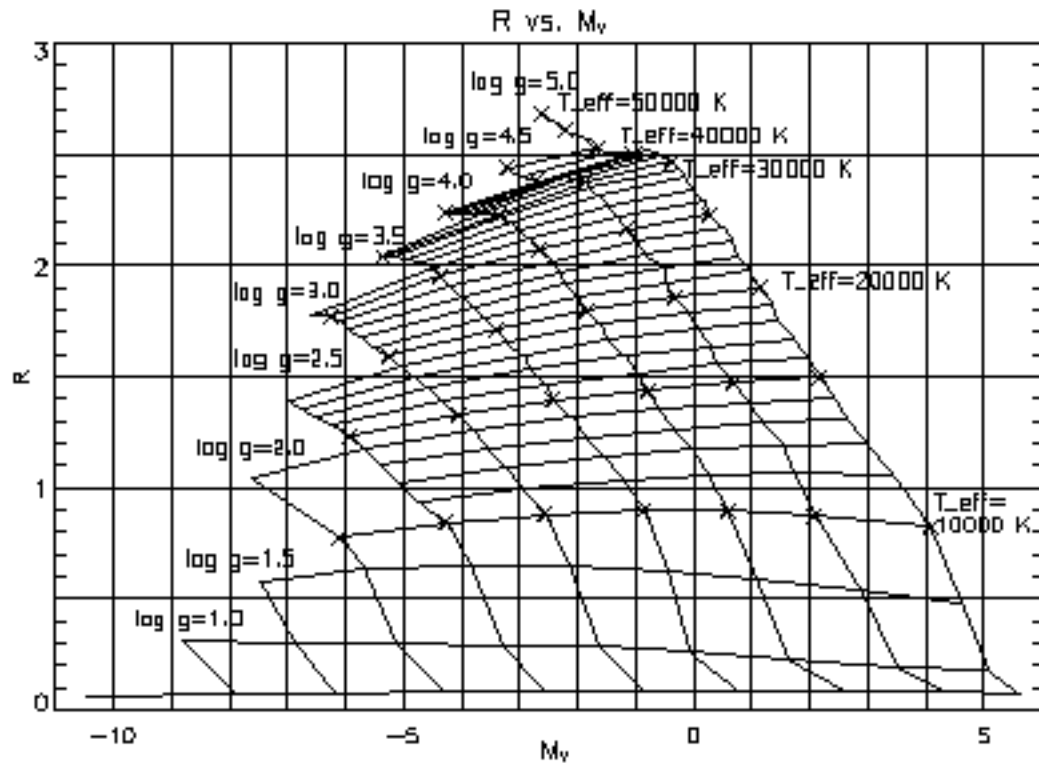


Figure 8: The calibration of R and absolute magnitude with $\log g$ and effective temperature using the Kurucz (1979) model atmospheres for one-third solar metallicity.

12,000 K). The atmospheres with the same $\log g$ move to the left and upwards when absolute magnitude decreases. There is not much difference between Figures 7 and 8, except Kurucz calculated fewer models for the one-third solar metallicity atmospheres (Figure 8).

3.2 Discussion of the Results of the Calculation of R for the Model Atmospheres

The values of R derived for the 24 Kunze model atmospheres for six values of metallicity can be found in Table 1. However, there is not much variation of R with metallicity for a given effective temperature and surface gravity. For the Kurucz models there is as much as a ten percent difference in R between atmospheres of solar metallicity and one-third solar metallicity.

The overall difference between Figure 7 and 8 is not that great when you consider other sources of error. For some stars with T_{eff} near 25,000 K and $\log g = 2.0$, you could have a 2,000 K difference in the results for T_{eff} , and sometimes a small change in $\log g$ as well. Since the LMC's metallicity is near one-third solar, we only used Figure 8 for our study of LMC stars in the next chapter.

We can now observe a sample of stars with a known distance, calculate R's and absolute magnitudes (from apparent magnitude) for each star. Then plot each star using one of the figures of this chapter to determine their corresponding values of effective temperature and surface gravity. In the next chapter we will use this to derive the masses for LMC stars.

CHAPTER IV

THE INITIAL MASS FUNCTION FOR MASSIVE STARS IN THE LMC

In this chapter we determine the massive star IMF using existing ultraviolet spectrophotometry of OB stars in the Large Magellanic Cloud. We begin by using the calibration of Figure 8 and this UV spectrophotometry to determine the effective temperatures and surface gravities of the LMC stars. Then we derive stellar masses, calculate the IMF of the LMC, and its slope.

4.1 Correcting for the Effects of Interstellar Absorption

To properly calculate R for each star using IUE spectra, each image has to be corrected for the effects of interstellar absorption. A major source of error in determining R is the color excess, $E(B-V)$. Oestreicher and Schmidt-Kaler (1996) point out that the LMC does not have an even dust distribution, and some stars have color excesses as high as 0.8. For stars located in 30 Doradus we will use individual color excesses for each star. However, for the purpose of this project we choose to use an average color excess for non-30 Dor stars. Naturally, this can introduce error in determining R for individual stars.

To de-redden the IUE images, we corrected for the galactic reddening using the extinction law of Savage and Mathis (1979) and an average $E(B-V)$ of 0.07 from Harris et al. (1997), who based their result on Oestreicher et al. (1995). We then corrected for the LMC reddening. For the non-30 Dor stars we used the non-30 Dor extinction law of

Fitzpatrick (1985) and an average $E(B-V)$ of 0.13 from Harris et al. (1997). For the 30 Doradus stars we identified, we de-reddened the images using the 30 Dor extinction law of Fitzpatrick (1985), and when available used the individual $E(B-V)$ from Fitzpatrick for each star (Table 12). The images were corrected using standard routines provided by the IUE Regional Data Analysis Facility (RDAF).

Table 12 Color excess for 30 Dor stars

Name	$E(B-V)_{lmc}$
SK -69 199	0.17
SK -68 126	0.09
SK -68 129	0.17
SK -69 265	0.17
HDE269997	0.19
SK -69 282	0.11
SK -68 155	0.19

4.2 Using the Stellar Temperature and Surface Gravity Calibration

The figures developed in Chapter 3 are for plotting a star's R and absolute magnitude to determine the T_{eff} and $\log g$, by interpolating the best one can. Absolute magnitude can be derived for each star from the distance modulus (DM), absorption (A_V ; in magnitudes), and apparent magnitude (m_V ; from Simbad, operated at CDS, Observatoire de Strasbourg), using the relation

$$M_V = m_V - DM - A_V . \quad (26)$$

From Westerlund (1990) we adopt 18.5 for the distance modulus to the LMC, and from Mateo and Hodge (1987) we adopt an average absorption of 0.25 magnitudes. However, since the dust distribution of the LMC is uneven, using an average value for the absorption will cause error in deriving absolute magnitude for some stars (Westerlund et al. 1995). This does effect the derivation of mass. However, you can

easily show that a small error in absolute magnitude has little effect on deriving the effective temperature and $\log g$ from Figure 8.

To illustrate this process in general, the star SK -68 41 has a de-reddened R value of 1.59 and an apparent magnitude of 12.01 from Simbad. From equation 26 the absolute magnitude is -6.99. If we plot R and absolute magnitude in Figure 8, and extrapolate, we find that $T_{\text{eff}} = 23,100$ K and $\log g = 2.69$.

4.3 Determining the Mass of a Star from LMC Data

Given the effective temperature, surface gravity, and bolometric magnitude for a star, it is a simple matter to determine the mass using

$$M_{\text{bol}_1} - M_{\text{bol}_{\text{sun}}} = -2.5 \log (L_1 / L_{\text{sun}}). \quad (27)$$

Since $L = 4\pi\mathcal{R}^2 \int F_{\lambda} d\lambda$, then

$$M_{\text{bol}_1} - M_{\text{bol}_{\text{sun}}} = -2.5 \log \frac{4\pi\mathcal{R}_1^2 \int F_{\lambda}^{(1)} d\lambda}{4\pi\mathcal{R}_{\text{sun}}^2 \int F_{\lambda}^{\text{sun}} d\lambda}. \quad (28)$$

With $\mathcal{R}^2 = GM / g$ and $\int F_{\lambda} d\lambda = \sigma T_{\text{eff}}^4$, then

$$M_{\text{bol}_1} - M_{\text{bol}_{\text{sun}}} = -2.5 \log \frac{4\pi GM_1 \sigma T_1^4 / g_1}{4\pi GM_{\text{sun}} \sigma T_{\text{sun}}^4 / g_{\text{sun}}}, \quad (29)$$

which simplifies to

$$M_{\text{bol}_1} - M_{\text{bol}_{\text{sun}}} = -2.5 \log \frac{\mathcal{M}_1 T_1^4 / g_1}{\mathcal{M}_{\text{sun}} T_{\text{sun}}^4 / g_{\text{sun}}}. \quad (30)$$

Finally, we find the mass to be

$$\mathcal{M}_1 = \frac{\mathcal{M}_{\text{sun}} T_{\text{sun}}^4 g_1}{T_1^4 g_{\text{sun}}} 10^{-0.4(M_{\text{bol}_1} - M_{\text{bol}_{\text{sun}}})}. \quad (31)$$

From Allen (2000) we adopt 5777 K for the effective temperature of the sun, 27400 cm/s^2 for the solar surface gravity, and 4.74 for the solar bolometric magnitude.

4.4 Stellar Parameter Results

Once effective temperature is found using Figure 8, we find the bolometric correction from Humphreys and McElroy (1984) and then the bolometric magnitude by combining equations 2 and 26:

$$M_{\text{bol}} = m_V - DM - A_V + \text{B.C.}, \quad (32)$$

where B.C. is usually negative. Table 13 shows apparent magnitudes (from Simbad) and then the derived stellar parameters for the 156 LMC stars studied in this thesis.

In Table 13 the star names are those listed in the IUE observing log; however, most of the stars have more than one name. Appendix B lists each star and gives some of the more popular names in use along with IUE image numbers and the spectral type from both the observing log and Simbad. Of the original 230 stars, slightly over 50 stars were either emission line stars or had bad spectra, and ten stars were not close enough to the graph for us to justify extrapolation. Table 14 compares our derived parameters with some of those found in the literature.

4.5 Determining Initial Mass Function for LMC

In order to compare results we define the initial mass function, $\log \Psi(M)$, to be the number of stars per kpc^2 per year per $\log (M/M_{\text{sun}})$, taking the area of the LMC to be 36.32 kpc^2 , from Humphreys and McElroy (1984). The mass range ages (T; main sequence lifetimes) come from Humphreys and McElroy as well. Humphreys and McElroy have eight times the total number of stars as our sample mainly because the IUE archive does not contain all of the known stars in the LMC. Our sample does not

Table 13 Derived stellar parameters of LMC stars

IUE Image Name	m_V	R	M_V	T_{eff} (K)	log g (cgs)	BC	M_{bol}	Mass (solar)
HDE268654	10.49	0.595	-8.26	-	-	-	-	-
SK-69 08	11.52	0.907	-7.23	12200	1.92	-0.66	-7.89	17.22
HDE268605	11.3	1.642	-7.45	25100	2.67	-2.26	-9.70	28.61
HDE268718	10.777	0.389	-7.973	-	-	-	-	-
SK-66 01	11.662	1.187	-7.088	15700	2.26	-1.07	-8.16	17.53
SK-69 19	12.82	1.569	-5.93	20500	2.85	-1.72	-7.65	14.68
SK-68 05	13.63	2.417	-5.12	46400	4.14	-4.14	-9.26	48.19
SK-66 5	10.7	0.980	-8.05	13700	1.84	-0.82	-8.87	22.25
SK-68 08	11.018	0.990	-7.732	13500	1.91	-0.80	-8.53	20.27
SK-67 15	11.6	0.883	-7.15	11900	1.91	-0.63	-7.78	16.76
SK-69 32	12.13	1.059	-6.62	13500	2.21	-0.80	-7.42	14.53
SK-66 27	11.82	0.914	-6.93	12100	1.99	-0.65	-7.58	15.71
SK-69 43	11.983	1.365	-6.767	18200	2.5	-1.38	-8.15	16.71
SK-66 36	11.35	0.843	-7.4	11600	1.82	-0.59	-7.99	18.38
SK-69 45	12.351	1.468	-6.399	19600	2.67	-1.59	-7.99	15.91
SK-68 11	12.313	1.460	-6.437	19600	2.66	-1.59	-8.03	16.10
HDE268804	11.21	0.887	-7.54	12200	1.84	-0.66	-8.20	19.06
SK-69 52	11.4	1.207	-7.35	16200	2.23	-1.13	-8.48	19.49
SK-65 04	12.25	1.663	-6.5	23200	2.85	-2.01	-8.51	19.89
SK-67 27	12.108	1.044	-6.642	13300	2.19	-0.78	-7.42	14.72
SK-67 28	12.266	1.563	-6.484	21400	2.75	-1.82	-8.31	18.01
SK-65 15	12.222	1.398	-6.528	18500	2.58	-1.42	-7.95	15.71
SK-65 16	11.96	1.583	-6.79	22500	2.73	-1.94	-8.73	20.75
SK-70 30	12.11	0.936	-6.64	12100	2.07	-0.65	-7.29	14.46
SK-65 19	12.072	1.465	-6.678	19900	2.61	-1.64	-8.32	17.63
SK-68 23	12.81	1.133	-5.94	13800	2.42	-0.83	-6.77	11.89
SK-65 20	11.193	1.126	-7.557	15200	2.12	-1.00	-8.56	20.97
SK-65 21	12.22	1.700	-6.53	24200	2.89	-2.14	-8.67	21.23
SK-67 36	12.032	1.251	-6.718	16200	2.39	-1.13	-7.85	15.74
SK-68 26	11.644	1.837	-7.106	31100	3.03	-2.93	-10.04	37.99
SK-70 44	12.04	1.117	-6.71	14200	2.25	-0.88	-7.59	15.21
SK-66 50	10.6	0.923	-8.15	13100	1.76	-0.76	-8.91	22.84
SK-70 48	11.67	1.038	-7.08	13500	2.09	-0.80	-7.88	16.83
SK-67 39	11.803	0.753	-6.947	10200	1.8	-0.39	-7.33	16.00
SK-70 50	11.1	1.116	-7.65	15100	2.09	-0.99	-8.64	21.63
SK-70 51	11.96	0.951	-6.79	12400	2.06	-0.68	-7.47	15.15
SK-67239	12.1	0.899	-6.65	11800	2.04	-0.62	-7.27	14.59
SK-67 43	12.71	1.238	-6.04	15200	2.49	-1.00	-7.04	12.16
SK-68 39	12.01	1.157	-6.74	14800	2.29	-0.95	-7.69	15.53
SK-70 58	12.81	1.491	-5.94	19100	2.77	-1.51	-7.45	13.51
SK-70 60	13.85	2.258	-4.9	39400	3.98	-3.68	-8.58	34.30
NS 29-65	13.55	2.105	-5.2	-	-	-	-	-

Table 13b Continuation of Table 13

IUE Image Name	m_V	R	M_V	T_{eff} (K)	$\log g$ (cgs)	BC	M_{bol}	Mass (solar)
SK-68 41	12.01	1.592	-6.74	22400	2.74	-1.93	-8.67	20.44
NS 69-70	13.94	2.252	-4.81	38700	4.00	-3.64	-8.45	34.19
S-68 42	11.95	1.496	-6.80	20800	2.63	-1.75	-8.55	19.25
SK-68 45	12.03	1.609	-6.72	22700	2.76	-1.96	-8.68	20.51
SK-68 46	12.45	1.309	-6.30	16700	2.53	-1.19	-7.49	13.87
SK-70 78	11.1	1.390	-7.65	-	-	-	-	-
HDE269074	11.1	1.491	-7.65	-	-	-	-	-
SK-70 79	12.73	1.450	-6.02	18800	2.73	-1.46	-7.48	13.56
SK-70 80	12.412	1.269	-6.34	16100	2.48	-1.12	-7.46	13.83
SK-67 51	12.63	2.041	-6.12	35600	3.48	-3.36	-9.48	37.26
SK-68 58	12.01	1.061	-6.74	13500	2.18	-0.80	-7.54	15.14
SK-68 59	12.07	1.137	-6.68	14500	2.28	-0.92	-7.60	15.07
SK-68 62	11.77	0.928	-6.98	12200	1.99	-0.66	-7.64	16.07
SK-67 58	11.276	0.879	-7.47	12000	1.84	-0.64	-8.11	18.79
D 1-9	13.57	1.706	-5.18	21800	3.13	-1.86	-7.04	12.54
S 89	11.956	1.077	-6.79	13800	2.19	-0.83	-7.63	15.37
LMC S89	11.956	0.711	-6.79	9800	1.79	-0.31	-7.11	14.91
SK-67 66	11.55	1.004	-7.20	13200	2.03	-0.77	-7.97	17.38
SK-69 89	11.323	1.018	-7.43	13600	2.00	-0.81	-8.24	18.47
SK-70 85	12.3	1.373	-6.45	17800	2.56	-1.33	-7.78	14.93
SK-69 91	10.762	1.195	-7.99	16900	2.12	-1.22	-9.21	24.92
HDE269321	10.492	0.442	-8.26	-	-	-	-	-
S 96	9.721	0.498	-9.03	-	-	-	-	-
SK-65 40	11.5	1.203	-7.25	16000	2.24	-1.11	-8.36	18.68
SK-69100	11.1	0.944	-7.65	12900	1.88	-0.74	-8.39	19.81
HDE269357	12.1	2.279	-6.65	47600	3.71	-4.26	-10.91	73.90
SK-67 78	11	1.066	-7.75	14500	2.01	-0.92	-8.67	21.69
SK-69110	11.65	1.117	-7.10	-	-	-	-	-
SK-69111	12	1.027	-6.75	13200	2.15	-0.77	-7.52	15.13
R 93	12.61	2.183	-6.14	41800	0.71	-3.84	-9.98	52.77
SK-67 81	11.6	0.979	-7.15	12900	2.01	-0.74	-7.89	16.86
SK-67 84	11.95	1.045	-6.80	13600	2.17	-0.81	-7.61	15.34
SK-6872A	12.99	1.563	-5.76	20100	2.87	-1.67	-7.43	13.60
SK-67 90	11.378	1.317	-7.37	18300	2.35	-1.39	-8.76	20.47
SK-66 78	12.22	1.612	-6.53	22300	2.79	-1.92	-8.45	19.06
SK-71 23	11.58	0.928	-7.17	12300	1.95	-0.67	-7.84	17.07
SK-68 75	12.05	1.384	-6.70	18400	2.53	-1.41	-8.11	16.55
SK-66 79	11.5	1.010	-7.25	13400	2.03	-0.79	-8.04	17.48
SK-66 86	12.89	1.217	-5.86	14700	2.50	-0.94	-6.80	11.38
SK-66 88	12.7	0.868	-6.05	11000	2.12	-0.52	-6.57	12.25
SK-67108	12.525	2.161	-6.23	41600	3.66	-3.83	-10.06	51.37
LH58:14	14.06	1.540	-4.69	18400	3.06	-1.41	-6.10	8.80

Table 13c Continuation of Table 13

IUE Image Name	m_V	R	M_V	T_{eff} (K)	$\log g$ (cgs)	BC	M_{bol}	Mass (solar)
LH58:52A	12.4	1.918	-6.35	30600	3.23	-2.88	-9.23	30.41
LH58:10	13.71	1.108	-5.04	13000	2.6	-0.75	-5.79	9.20
LH58:30	13.52	2.335	-5.23	43900	4.03	-3.95	-9.18	43.17
SK-71 30	11.61	0.831	-7.14	11300	1.86	-0.56	-7.70	17.05
LH58:10A	13.1	2.277	-5.65	43200	3.89	-3.91	-9.56	47.55
SK-67112	11.9	1.653	-6.85	23700	2.78	-2.08	-8.93	22.72
SK-67116	11.1	1.170	-7.65	16000	2.14	-1.11	-8.76	21.45
-67 117A	B12.5	1.737	-18.75	24300	2.97	-2.15	-8.40	19.63
SK-67117	12.92	1.806	-5.83	25000	3.11	-2.24	-8.07	17.80
SK-69139	11.877	1.064	-6.873	13700	2.16	-0.82	-7.70	15.72
SK-66100	13.26	2.186	-5.49	38800	3.8	-3.64	-9.13	40.15
SK-67122	10.9	0.913	-7.85	12600	1.8	-0.70	-8.55	21.14
SK-68 87	11.83	1.076	-6.92	13800	2.16	-0.83	-7.75	16.11
SK-69143	10.81	0.708	-7.94	10200	1.54	-0.39	-8.33	21.95
SK-67126	11.1	1.002	-7.65	13600	1.94	-0.81	-8.46	19.76
SK-65 63	12.56	1.818	-6.19	26000	3.1	-2.36	-8.55	23.25
SK-68 92	11.71	1.256	-7.04	16700	2.34	-1.19	-8.23	17.70
SK-69149	11.3	0.947	-7.45	12800	1.92	-0.72	-8.17	18.46
SK-67130	11.51	0.892	-7.24	11900	1.89	-0.63	-7.87	17.38
SK-66106	12.72	1.401	-6.03	17800	2.67	-1.33	-7.36	13.06
SK-66107	12.87	1.311	-5.88	16100	2.6	-1.12	-7.00	11.96
HDE269619	11.2	0.551	-7.55	-	-	-	-	-
SK-67137	11.93	0.941	-6.82	12300	2.04	-0.67	-7.49	15.21
SK-67138	12.13	1.123	-6.62	14300	2.28	-0.89	-7.51	14.74
S-69 160	12.45	1.392	-6.3	18000	2.61	-1.35	-7.65	14.26
SK-69162	11.8	1.328	-6.95	17800	2.43	-1.33	-8.28	17.54
SK-66118	11.776	1.273	-6.974	16900	2.37	-1.22	-8.19	17.41
SK-67153	12.01	1.068	-6.74	13600	2.19	-0.81	-7.55	15.20
SK-69172	12.08	0.911	-6.67	11800	2.03	-0.62	-7.29	14.52
SK-67168	12.08	1.917	-6.67	32800	3.21	-3.13	-9.80	37.17
SK-67167	12.529	2.149	-6.221	41400	3.64	-3.82	-10.04	49.37
SK-69177	12.11	0.807	-6.64	10700	1.93	-0.47	-7.11	14.52
SK-67174	11.52	2.043	-7.23	-	-	-	-	-
SK-69179	11.71	1.037	-7.04	13500	2.1	-0.80	-7.84	16.60
S-67 177	11.57	1.276	-7.18	17200	2.34	-1.26	-8.44	18.93
SK-69181	11.93	0.994	-6.82	12900	2.1	-0.74	-7.56	15.31
S-67 179	12.676	1.481	-6.074	19200	2.74	-1.53	-7.60	14.18
SK-68121	12.133	1.044	-6.617	13200	2.19	-0.77	-7.39	14.68
SK-67191	13.46	2.028	-5.29	29500	3.49	-2.77	-8.06	21.88
SK-66143	11.75	1.005	-7	13100	2.07	-0.76	-7.76	16.17
S-67 197	12.3	0.980	-6.45	12500	2.16	-0.69	-7.14	13.63
SK-66152	12.49	1.916	-6.26	29500	3.22	-2.77	-9.03	28.71

Table 13d Continuation of Table 13

IUE Image Name	m_V	R	M_V	T_{eff} (K)	$\log g$ (cgs)	BC	M_{bol}	Mass (solar)
SK-69193	12.1	1.493	-6.65	20500	2.65	-1.72	-8.37	17.98
SK-67206	12	1.573	-6.75	22000	2.71	-1.88	-8.63	19.91
SK-69197	12.15	1.236	-6.6	15800	2.39	-1.08	-7.68	14.89
SK-69199	12.8	0.771	-5.95	12600	2.31	-0.70	-6.65	11.89
SK-67214	11.85	1.010	-6.9	13100	2.1	-0.76	-7.66	15.80
SK-69203	12.29	0.972	-6.46	12400	2.15	-0.68	-7.14	13.75
SK-69205	12.17	1.475	-6.58	20000	2.64	-1.66	-8.24	17.18
SK-67217	11.79	1.757	-6.96	26000	2.9	-2.36	-9.32	29.81
SK-68126	12.61	0.971	-6.14	12800	2.28	-0.72	-6.86	12.65
SK-69206	12.84	0.942	-5.91	11700	2.23	-0.60	-6.51	11.70
SK-66166	11.71	1.163	-7.04	15100	2.24	-0.99	-8.03	17.42
SK-67222	11.187	1.384	-7.563	19900	2.38	-1.64	-9.20	23.46
SK-67220	11.79	1.111	-6.96	14400	2.2	-0.90	-7.86	16.50
SK-68129	12.77	1.050	-5.98	17600	2.67	-1.30	-7.28	12.77
HDE269846	11.63	0.991	-7.12	13000	2.03	-0.75	-7.87	16.81
SK-66169	12.56	1.590	-6.19	21300	2.83	-1.81	-8.00	16.66
SK-66172	13.13	2.279	-5.62	43200	3.9	-3.91	-9.53	47.33
SK-66178	12.07	1.839	-6.68	28500	3.07	-2.68	-9.36	31.50
SK-67228	11.49	1.289	-7.26	17600	2.34	-1.30	-8.56	19.41
SK-69236	12.43	0.958	-6.32	12200	2.17	-0.66	-6.98	13.25
SK-69237	11.6	1.062	-7.15	-	-	-	-	-
R 133	12.35	1.518	-6.4	20500	2.72	-1.72	-8.12	16.78
SK-69252	12.35	0.862	-6.4	11200	2.04	-0.55	-6.95	13.38
SK-69261	12.16	0.700	-6.59	9600	1.82	-0.28	-6.87	13.88
SK-69264	11.67	0.509	-7.08	8700	1.56	-0.08	-7.16	14.81
SK-69265	11.88	0.644	-6.87	11300	1.93	-0.56	-7.43	15.62
HDE269997	11.27	0.657	-7.48	12500	1.88	-0.69	-8.17	18.48
SK-69271	11.8	1.096	-6.95	14100	2.18	-0.87	-7.82	16.42
SK-69276	12.406	1.564	-6.344	21200	2.78	-1.80	-8.14	17.27
SK-69282	12.06	0.972	-6.69	13900	2.23	-0.85	-7.54	15.03
SK-69290	12.21	1.211	-6.54	15400	2.38	-1.03	-7.57	14.54
SK-68155	12.72	1.030	-6.03	18500	2.71	-1.42	-7.45	13.40
SK-71 52	12.57	0.871	-6.18	11100	2.1	-0.53	-6.71	12.86
SK-67255	11.1	1.136	-7.65	15700	2.12	-1.07	-8.72	21.31
SK-67256	11.888	1.385	-6.862	18800	2.51	-1.46	-8.33	17.74
SK-67258	12.11	0.963	-6.64	12400	2.1	-0.68	-7.32	14.47
SK-70115	12.24	1.795	-6.51	26100	3.03	-2.38	-8.89	26.47
LH117:13	14.24	1.950	-4.51	25500	3.48	-2.30	-6.81	12.11
LH117:43	13	1.943	-5.75	28100	3.3	-2.63	-8.38	23.09
LH117:11	13.15	2.158	-5.6	38200	3.76	-3.61	-9.21	41.81
SK-68171	12.03	1.450	-6.72	19700	2.59	-1.61	-8.33	17.69

Table 14 Comparison of derived stellar parameters

IUE Image Name	Derived Parameters			Comparison Parameters			Reference
	T _{eff} (K)	log g (cgs)	Mass (solar)	T _{eff} (K)	Log g (cgs)	Mass (solar)	
SK -66 172	43,200	3.90	47.33	50,000	4.2	---	(1)
NS 69-70	38,700	4.00	34.19	46,500	4.1	---	(1)
SK -65 21	24,200	2.89	21.23	27,000	2.7	16	(2)
SK -68 41	22,400	2.74	20.44	25,000	2.6	15	(2)
SK -68 41	22,400	2.74	20.44	22,200	2.7	18	(3)
SK -67 90	18,300	2.35	20.47	17,900	2.2	17	(3)
SK -67 78	14,500	2.01	21.69	14,000	1.7	9	(3)
SK -67 256	18,800	2.51	17.74	19,600	2.3	10	(3)
HDE 268605	25,100	2.67	28.61	26,000	---	---	(4)
SK -66 01	15,700	2.26	17.53	17,500	---	---	(4)
SK -66 50	13,100	1.76	22.84	13,500	---	---	(4)
SK -66 05	13,700	1.84	22.25	14,500	---	---	(4)
SK -68 08	13,500	1.91	20.27	14,000	---	---	(4)
SK -69 43	18,200	2.50	16.71	21,000	---	---	(4)
SK -68 58	13,500	2.18	15.14	13,500	---	---	(4)
SK -71 23	12,300	1.95	17.07	13,500	---	---	(4)
SK -67 126	13,600	1.94	19.76	13,500	---	---	(4)
SK -67 130	11,900	1.89	17.38	12,500	---	---	(4)
HDE 269997	12,500	1.88	18.48	14,500	---	---	(4)

Reference (1) is from Gehren et al. (1986), (2) is Kudritzki et al. (1989), (3) is Fitzpatrick (1987), and (4) is from van Genderen (1983).

contain all of the LMC stars in the IUE archive as well. Therefore, we shall correct for completeness by multiplying our results by eight, and use the following relation for the IMF:

$$\log \Psi(M) = \log \{ N \text{ Area}^{-1} T^{-1} [\Delta \log (M)]^{-1} \}. \quad (33)$$

Table 15 shows how $\log \Psi(M)$ is calculated.

Table 15 Calculating $\log \Psi(M)$ per solar mass interval

Mass Range (solar masses)	N	N (corrected)	Area (kpc ²)	T (years)	$\Delta \log (M)$ (solar masses)	$\log \Psi(M)$ This Thesis
60-85	1	8	36.32	3.5×10^6	0.15	-6.38
30-60	16	128	36.32	5.3×10^6	0.30	-5.66
15-30	96	768	36.32	9.2×10^6	0.30	-5.12
9-15	43	344	36.32	18.0×10^6	0.22	-5.62
Total N	156	1248				

Table 16 compares the results with those of Humphreys and McElroy (1984) and shows the steps needed to plot $\log \Psi(M)$ with $\log (M/M_{\text{sun}})$, which is the log average of the mass range, in Figure 9.

Table 16 Number and $\log \Psi(M)$ per solar mass interval

Mass Range (solar masses)	$\log (M/M_{\text{sun}})$ (solar masses)	N Corrected This Thesis	N Humphreys ¹	$\log \Psi(M)$ This Thesis	$\log \Psi(M)$ Humphreys ¹
85-120	2.00	0	9	-	-6.26
60-85	1.85	8	33	-6.38	-5.76
30-60	1.61	128	254	-5.66	-5.31
15-30	1.31	768	746	-5.12	-5.13
9-15	1.06	344	201	-5.62	-5.99
Total N		1248	1273		

(1) Humphreys and McElroy (1984)

In Figure 9 the initial mass function, $\log \Psi(M)$, is shown as a function of $\log (M/M_{\text{sun}})$. The slope for the mass range $85 M_{\text{sun}} \geq M \geq 15 M_{\text{sun}}$ is $\Gamma = -2.31$, and it was derived using the method of least squares. This result is within the range of others found in the literature (Scalo 1986b).

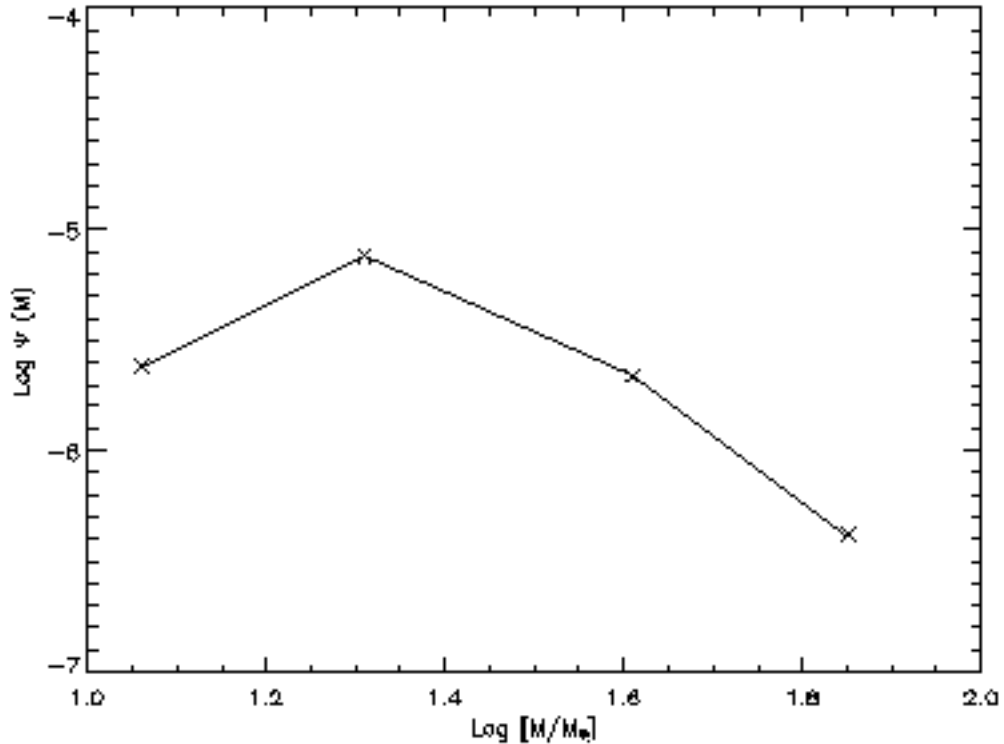


Figure 9: The initial mass function $\log \Psi(M)$ vs. $\log (M/M_{\text{sun}})$ for the LMC

4.6 Conclusions

The original purpose of this thesis was to see if R could be related to the effective surface temperatures of stars whose distances are well known. It was learned that R and absolute magnitude of a star could be correlated with effective temperature and surface gravity by use of stellar atmospheres and evolutionary tracks. From IUE spectra, absolute magnitude, and Figure 8, we derived the effective temperatures, surface gravities, and masses for 156 LMC stars. Then we derived the initial mass function and its slope.

The values of R derived for the 144 Kunze model atmospheres are shown in Table 2. However, there is not much variation of R with metallicity for a given effective temperature and surface gravity. Table 1 shows the results for R as a function of T_{eff} and $\log g$ for the 24 Kunze model atmospheres with solar metallicity. Table 3 shows the results for R as a function of T_{eff} and $\log g$ for the 218 Kurucz model atmospheres with solar metallicity, and Table 4 shows R for Kurucz atmospheres with one-third solar metallicity. Tables 9 and 10 show absolute magnitude as a function of T_{eff} and $\log g$ for the Kunze and Kurucz model atmospheres with solar metallicity, respectively. Table 11 shows absolute magnitudes for Kurucz model atmospheres with one-third solar metallicity. Figures 6-8 graphically show how R varies with T_{eff} and with absolute magnitude for each set of atmospheres. Table 13 shows the derived T_{eff} , $\log g$, and mass for each of our sample of LMC stars. Table 14 shows comparisons of our derived parameters with others found in the literature. Table 15 shows how $\log \Psi(M)$ was derived, and Figure 9 shows the graph of the initial mass function. The slope of the initial mass function for the mass range $85 M_{\text{sun}} \geq M \geq 15 M_{\text{sun}}$ was found to be $\Gamma = -2.31$.

This work was felt to be important because of the need to find a more accurate method for determining the IMF for objects like the LMC whose distance is well known. A better understanding of the IMF is important for the future study of galactic evolution.

REFERENCES

- Allen , C. W., 2000, *Astrophysical Quantities*, 4rd Ed., Springer-Verlag, New York, p. 350
- Allen , C. W., 1973, *Astrophysical Quantities*, 3rd Ed., Athlone Press, London, p. 201
- Boggess, A., Carr, F. A., Evans, D. C., Fischel, D., Freeman, H. R., Fuechsel, C. F., KlingleSmith, D. A., Krueger, V. L., Longanecker, G. W., Moore, J. V., 1978, *Nature*, **275**, 372
- Collins, G. W., 1989, *The Fundamentals of Stellar Astrophysics*, W. H. Freeman and Co, New York, p. 400
- Fitzpatrick, E.L., 1985, *ApJ*, **299**, 219
- Fitzpatrick, E.L., 1987, *ApJ*, **312**, 596
- Gehren, T., Husfeld, D., Kudritzki, R. P., Conti, P. S., Hummer, D. G., 1986, *Luminous Stars and Associations in Galaxies, IAU Colloq. No. 116*, ed. C. W. H. De Loore et al, pp. 413-414. Dordrecht, D Reidel Publishing Co., 533 pp.
- Harris, J., Zaritsky, D., and Thompson, I., 1997, *AJ*, **114**, 1933
- Hill, R., Madore, B. F., and Freedman, W. L., 1994a, *ApJS*, **91**, 583
- Hill, R., Madore, B. F., and Freedman, W. L., 1994b, *ApJ*, **429**, 192
- Hill, R., Madore, B. F., and Freedman, W. L., 1994c, *ApJ*, **429**, 204
- Humphreys, R. M., and McElroy, D. B., 1984, *ApJ*, **284**, 565
- Iben, I., Jr., 1967 *ARAA*, **5**, 571
- Kudritzki, R. P., Gabler, A., Gabler, R., Groth, H. G., Pauldrach, A., and Puls, J., 1989, *Physics of Luminous Blue Variables, IAU Colloq. No. 113*, ed. K. Davidson, A. F. J. Moffat, H. J. G. L. M. Lamers, pp. 67-80. Dordrecht: Kluwer. 328 pp.
- Kunze, D., 1994, Ph.D. thesis, Universitaets-Sternwarte Muenchen
- Kurucz, R., L., 1979, *ApJS*, **40**, 1

- Mateo, M., and Hodge, P., 1987, APJ, **320**, 626
- Massey, P., Garmany, C. D., Silkey, M., and Degioia-Eastwood, K., 1989a, AJ, **97**, 107
- Massey, P., Parker, J. W., and Garmany, C. D., 1989b, AJ, **98**, 1305
- Mihalas, D., 1978, *Stellar Atmospheres*, W. H. Freeman and Co, San Francisco, p.403
- Oestreicher, M. O., and Schmidt-Kaler, T., 1996, A&AS, **117**, 103
- Oestreicher, M. O., Gochermann, J., and Schmidt-Kaler, T., 1995, A&AS, **112**, 495
- Savage, B. D., and Mathis, J. S., 1979, Ann. Rev. A&A, **17**, 73
- Scalo, J. M., 1986a, Fund. Cos. Phys., **11**, 1
- Scalo, J. M., 1986b, *Luminous Stars and Associations in Galaxies*, IAU Colloq. No. 116, ed. C. W. H. De Loore et al, pp. 451-456. Dordrecht, D Reidel Publishing Co., 533 pp.
- Schaerer, D., Meynet, G., Maeder, A., and Schaller, G., 1993, A&AS, **98**, 523
- Shu, F. H., 1982, *The Physical Universe*, University Science Books, Mill Valley, California, p. 166
- van Genderen, A. M., Groot, M., and The, P.S., 1983, A&A, **117**, 53
- Walborn, N. R., Mackenty, J. W., Saha, A., White, R. L., and Parker, J. W., 1995, ApJ (Letters), **439**, L47
- Westerlund, B. E., 1990, A&AR, **2**, 29
- Westerlund, B. E., Linde, P., Lynga, G., 1995, A&A, **298**, 39

APPENDIX A

DERIVED BOLOMETRIC MAGNITUDES FOR EACH ATMOSPHERE AND FOR EACH MASS OF THE EVOLUTIONARY TRACKS

Solar Mass	T_eff log g	6,000 K 4.50	6,000 K 4.00	6,000 K 3.50	6,000 K 3.00	6,000 K 2.50	6,000 K 2.00
120		-0.467	-1.717	-2.967	-4.217	-5.467	-6.717
85		-0.092	-1.342	-2.592	-3.842	-5.092	-6.342
60		0.286	-0.964	-2.214	-3.464	-4.714	-5.964
40		0.726	-0.524	-1.774	-3.024	-4.274	-5.524
25		1.236	-0.014	-1.264	-2.514	-3.764	-5.014
20		1.478	0.228	-1.022	-2.272	-3.522	-4.772
15		1.791	0.541	-0.709	-1.959	-3.209	-4.459
12		2.033	0.783	-0.467	-1.717	-2.967	-4.217
10		2.231	0.981	-0.269	-1.519	-2.769	-4.019
7		2.618	1.368	0.118	-1.132	-2.382	-3.632
5		2.984	1.734	0.484	-0.766	-2.016	-3.266
4		3.226	1.976	0.726	-0.524	-1.774	-3.024
3		3.538	2.288	1.038	-0.212	-1.462	-2.712
2.5		3.736	2.486	1.236	-0.014	-1.264	-2.514
2		3.978	2.728	1.478	0.228	-1.022	-2.272

Solar Mass	T_eff log g	6,000 K 1.50	6,000 K 1.00	6,000 K 0.50	6,000 K 0.00	7,000 K 5.00	7,000 K 4.50
120		-7.967	-9.217	-10.468	-11.717	0.114	-1.136
85		-7.593	-8.842	-10.093	-11.342	0.488	-0.762
60		-7.214	-8.464	-9.715	-10.964	0.866	-0.384
40		-6.774	-8.024	-9.275	-10.524	1.306	0.056
25		-6.264	-7.514	-8.765	-10.014	1.817	0.567
20		-6.022	-7.272	-8.522	-9.772	2.059	0.809
15		-5.709	-6.959	-8.210	-9.459	2.371	1.121
12		-5.467	-6.717	-7.968	-9.217	2.614	1.364
10		-5.269	-6.519	-7.770	-9.019	2.812	1.562
7		-4.882	-6.132	-7.382	-8.632	3.199	1.949
5		-4.516	-5.766	-7.017	-8.266	3.564	2.314
4		-4.274	-5.524	-6.775	-8.024	3.806	2.556
3		-3.962	-5.212	-6.463	-7.712	4.119	2.869
2.5		-3.764	-5.014	-6.265	-7.514	4.317	3.067
2		-3.522	-4.772	-6.022	-7.272	4.559	3.309

Solar Mass	T_eff log g	7,000 K 4.00	7,000 K 3.50	7,000 K 3.00	7,000 K 2.50	7,000 K 2.00	7,000 K 1.50
120		-2.386	-3.636	-4.886	-6.136	-7.386	-8.636
85		-2.012	-3.262	-4.512	-5.762	-7.012	-8.262
60		-1.634	-2.884	-4.134	-5.384	-6.634	-7.884
40		-1.194	-2.444	-3.694	-4.944	-6.194	-7.444
25		-0.683	-1.933	-3.183	-4.433	-5.683	-6.933
20		-0.441	-1.691	-2.941	-4.191	-5.441	-6.691
15		-0.129	-1.379	-2.629	-3.879	-5.129	-6.379
12		0.114	-1.136	-2.386	-3.636	-4.886	-6.136
10		0.312	-0.938	-2.188	-3.438	-4.688	-5.939
7		0.699	-0.551	-1.801	-3.051	-4.301	-5.551
5		1.064	-0.186	-1.436	-2.686	-3.936	-5.186
4		1.306	0.056	-1.194	-2.444	-3.694	-4.944
3		1.619	0.369	-0.881	-2.131	-3.381	-4.631
2.5		1.817	0.567	-0.683	-1.933	-3.183	-4.433
2		2.059	0.809	-0.441	-1.691	-2.941	-4.191

Solar Mass	T_eff log g	7,000 K 1.00	7,000 K 0.50	8,000 K 5.00	8,000 K 4.50	8,000 K 4.00	8,000 K 3.50
120		-9.886	-11.137	-0.466	-1.716	-2.966	-4.216
85		-9.512	-10.763	-0.092	-1.342	-2.592	-3.842
60		-9.134	-10.385	0.286	-0.964	-2.214	-3.464
40		-8.694	-9.944	0.727	-0.523	-1.773	-3.023
25		-8.183	-9.434	1.237	-0.013	-1.263	-2.513
20		-7.941	-9.192	1.479	0.229	-1.021	-2.271
15		-7.629	-8.879	1.791	0.541	-0.709	-1.959
12		-7.386	-8.637	2.034	0.784	-0.466	-1.716
10		-7.188	-8.439	2.232	0.982	-0.268	-1.518
7		-6.801	-8.052	2.619	1.369	0.119	-1.131
5		-6.436	-7.687	2.984	1.734	0.484	-0.766
4		-6.194	-7.444	3.227	1.977	0.727	-0.523
3		-5.881	-7.132	3.539	2.289	1.039	-0.211
2.5		-5.683	-6.934	3.737	2.487	1.237	-0.013
2		-5.441	-6.692	3.979	2.729	1.479	0.229

Solar Mass	T_eff log g	8,000 K 3.00	8,000 K 2.50	8,000 K 2.00	8,000 K 1.50	8,000 K 1.00	9,000 K 5.00
120		-5.466	-6.716	-7.966	-9.216	-10.466	-0.978
85		-5.092	-6.342	-7.592	-8.842	-10.092	-0.603
60		-4.714	-5.964	-7.214	-8.464	-9.714	-0.225
40		-4.273	-5.523	-6.773	-8.024	-9.273	0.215
25		-3.763	-5.013	-6.263	-7.513	-8.763	0.725
20		-3.521	-4.771	-6.021	-7.271	-8.521	0.968
15		-3.209	-4.459	-5.709	-6.959	-8.209	1.280
12		-2.966	-4.216	-5.466	-6.716	-7.966	1.522
10		-2.768	-4.018	-5.268	-6.518	-7.768	1.720
7		-2.381	-3.631	-4.881	-6.131	-7.381	2.107
5		-2.016	-3.266	-4.516	-5.766	-7.016	2.473
4		-1.773	-3.023	-4.273	-5.524	-6.773	2.715
3		-1.461	-2.711	-3.961	-5.211	-6.461	3.027
2.5		-1.263	-2.513	-3.763	-5.013	-6.263	3.225
2		-1.021	-2.271	-3.521	-4.771	-6.021	3.468

Solar Mass	T_eff log g	9,000 K 4.50	9,000 K 4.00	9,000 K 3.50	9,000 K 3.00	9,000 K 2.50	9,000 K 2.00
120		-2.228	-3.478	-4.728	-5.978	-7.228	-8.478
85		-1.853	-3.103	-4.353	-5.603	-6.853	-8.103
60		-1.475	-2.725	-3.975	-5.225	-6.475	-7.725
40		-1.035	-2.285	-3.535	-4.785	-6.035	-7.285
25		-0.525	-1.775	-3.025	-4.275	-5.525	-6.775
20		-0.282	-1.532	-2.782	-4.032	-5.282	-6.532
15		0.030	-1.220	-2.470	-3.720	-4.970	-6.220
12		0.272	-0.978	-2.228	-3.478	-4.728	-5.978
10		0.470	-0.780	-2.030	-3.280	-4.530	-5.780
7		0.857	-0.393	-1.643	-2.893	-4.143	-5.393
5		1.223	-0.027	-1.277	-2.527	-3.777	-5.027
4		1.465	0.215	-1.035	-2.285	-3.535	-4.785
3		1.777	0.527	-0.723	-1.973	-3.223	-4.473
2.5		1.975	0.725	-0.525	-1.775	-3.025	-4.275
2		2.218	0.968	-0.282	-1.532	-2.782	-4.032

Solar Mass	T_eff log g	9,000 K 1.50	10,000 K 5.00	10,000 K 4.50	10,000 K 4.00	10,000 K 3.50	10,000 K 3.00
120		-9.728	-1.435	-2.685	-3.935	-5.185	-6.435
85		-9.353	-1.061	-2.311	-3.561	-4.811	-6.061
60		-8.975	-0.683	-1.933	-3.183	-4.433	-5.683
40		-8.535	-0.243	-1.493	-2.743	-3.993	-5.243
25		-8.025	0.268	-0.982	-2.232	-3.482	-4.732
20		-7.783	0.510	-0.740	-1.990	-3.240	-4.490
15		-7.470	0.822	-0.428	-1.678	-2.928	-4.178
12		-7.228	1.065	-0.185	-1.435	-2.685	-3.935
10		-7.030	1.263	0.013	-1.237	-2.487	-3.737
7		-6.643	1.650	0.400	-0.850	-2.100	-3.350
5		-6.277	2.015	0.765	-0.485	-1.735	-2.985
4		-6.035	2.257	1.007	-0.243	-1.493	-2.743
3		-5.723	2.570	1.320	0.070	-1.180	-2.430
2.5		-5.525	2.768	1.518	0.268	-0.982	-2.232
2		-5.283	3.010	1.760	0.510	-0.740	-1.990

Solar Mass	T_eff log g	10,000 K 2.50	10,000 K 2.00	11,000 K 5.00	11,000 K 4.50	11,000 K 4.00	11,000 K 3.50
120		-7.685	-8.935	-1.849	-3.099	-4.349	-5.599
85		-7.311	-8.561	-1.475	-2.725	-3.975	-5.225
60		-6.933	-8.183	-1.097	-2.347	-3.597	-4.847
40		-6.493	-7.743	-0.657	-1.907	-3.157	-4.407
25		-5.982	-7.232	-0.146	-1.396	-2.646	-3.896
20		-5.740	-6.990	0.096	-1.154	-2.404	-3.654
15		-5.428	-6.678	0.408	-0.842	-2.092	-3.342
12		-5.185	-6.435	0.651	-0.599	-1.849	-3.099
10		-4.987	-6.237	0.849	-0.401	-1.651	-2.901
7		-4.600	-5.850	1.236	-0.014	-1.264	-2.514
5		-4.235	-5.485	1.601	0.351	-0.899	-2.149
4		-3.993	-5.243	1.843	0.593	-0.657	-1.907
3		-3.680	-4.930	2.156	0.906	-0.344	-1.594
2.5		-3.482	-4.732	2.354	1.104	-0.146	-1.396
2		-3.240	-4.490	2.596	1.346	0.096	-1.154

Solar Mass	T_eff log g	11,000 K 3.00	11,000 K 2.50	11,000 K 2.00	12,000 K 5.00	12,000 K 4.50	12,000 K 4.00
120		-6.849	-8.099	-9.349	-2.227	-3.477	-4.727
85		-6.475	-7.725	-8.975	-1.853	-3.103	-4.353
60		-6.097	-7.347	-8.597	-1.475	-2.725	-3.975
40		-5.657	-6.906	-8.157	-1.034	-2.284	-3.534
25		-5.146	-6.396	-7.646	-0.524	-1.774	-3.024
20		-4.904	-6.154	-7.404	-0.282	-1.532	-2.782
15		-4.592	-5.842	-7.092	0.031	-1.219	-2.469
12		-4.349	-5.599	-6.849	0.273	-0.977	-2.227
10		-4.151	-5.401	-6.651	0.471	-0.779	-2.029
7		-3.764	-5.014	-6.264	0.858	-0.392	-1.642
5		-3.399	-4.649	-5.899	1.223	-0.027	-1.277
4		-3.157	-4.406	-5.657	1.466	0.216	-1.034
3		-2.844	-4.094	-5.344	1.778	0.528	-0.722
2.5		-2.646	-3.896	-5.146	1.976	0.726	-0.524
2		-2.404	-3.654	-4.904	2.218	0.968	-0.282

Solar Mass	T_eff log g	12,000 K 3.50	12,000 K 3.00	12,000 K 2.50	12,000 K 2.00	13,000 K 5.00	13,000 K 4.50
120		-5.977	-7.227	-8.477	-9.727	-2.575	-3.825
85		-5.603	-6.853	-8.103	-9.353	-2.200	-3.450
60		-5.225	-6.475	-7.725	-8.975	-1.822	-3.072
40		-4.784	-6.034	-7.284	-8.534	-1.382	-2.632
25		-4.274	-5.524	-6.774	-8.024	-0.872	-2.122
20		-4.032	-5.282	-6.532	-7.782	-0.629	-1.879
15		-3.719	-4.969	-6.219	-7.469	-0.317	-1.567
12		-3.477	-4.727	-5.977	-7.227	-0.075	-1.325
10		-3.279	-4.529	-5.779	-7.029	0.123	-1.127
7		-2.892	-4.142	-5.392	-6.642	0.510	-0.740
5		-2.527	-3.777	-5.027	-6.277	0.876	-0.374
4		-2.284	-3.534	-4.784	-6.034	1.118	-0.132
3		-1.972	-3.222	-4.472	-5.722	1.430	0.180
2.5		-1.774	-3.024	-4.274	-5.524	1.628	0.378
2		-1.532	-2.782	-4.032	-5.282	1.871	0.621

Solar Mass	T_eff log g	13,000 K 4.00	13,000 K 3.50	13,000 K 3.00	13,000 K 2.50	13,000 K 2.00	14,000 K 5.00
120		-5.075	-6.325	-7.575	-8.825	-10.075	-2.897
85		-4.700	-5.950	-7.200	-8.450	-9.700	-2.522
60		-4.322	-5.572	-6.822	-8.072	-9.322	-2.144
40		-3.882	-5.132	-6.382	-7.632	-8.882	-1.704
25		-3.372	-4.622	-5.872	-7.122	-8.372	-1.194
20		-3.129	-4.379	-5.629	-6.879	-8.129	-0.951
15		-2.817	-4.067	-5.317	-6.567	-7.817	-0.639
12		-2.575	-3.825	-5.075	-6.325	-7.575	-0.397
10		-2.377	-3.627	-4.877	-6.127	-7.377	-0.199
7		-1.990	-3.240	-4.490	-5.740	-6.990	0.189
5		-1.624	-2.874	-4.124	-5.374	-6.624	0.554
4		-1.382	-2.632	-3.882	-5.132	-6.382	0.796
3		-1.070	-2.320	-3.570	-4.820	-6.070	1.108
2.5		-0.872	-2.122	-3.372	-4.622	-5.872	1.306
2		-0.629	-1.879	-3.129	-4.379	-5.629	1.549

Solar Mass	T_eff log g	14,000 K 4.50	14,000 K 4.00	14,000 K 3.50	14,000 K 3.00	14,000 K 2.50	14,000 K 2.00
120		-4.147	-5.397	-6.647	-7.897	-9.147	-10.397
85		-3.772	-5.022	-6.272	-7.522	-8.772	-10.022
60		-3.394	-4.644	-5.894	-7.144	-8.394	-9.644
40		-2.954	-4.204	-5.454	-6.704	-7.954	-9.204
25		-2.444	-3.694	-4.944	-6.194	-7.444	-8.694
20		-2.201	-3.451	-4.701	-5.951	-7.201	-8.451
15		-1.889	-3.139	-4.389	-5.639	-6.889	-8.139
12		-1.647	-2.897	-4.147	-5.397	-6.647	-7.897
10		-1.449	-2.699	-3.949	-5.199	-6.449	-7.699
7		-1.061	-2.311	-3.561	-4.811	-6.061	-7.311
5		-0.696	-1.946	-3.196	-4.446	-5.696	-6.946
4		-0.454	-1.704	-2.954	-4.204	-5.454	-6.704
3		-0.142	-1.392	-2.642	-3.892	-5.142	-6.392
2.5		0.056	-1.194	-2.444	-3.694	-4.944	-6.194
2		0.299	-0.951	-2.201	-3.451	-4.701	-5.951

Solar Mass	T_eff log g	15,000 K 5.00	15,000 K 4.50	15,000 K 4.00	15,000 K 3.50	15,000 K 3.00	15,000 K 2.50
120		-3.196	-4.446	-5.696	-6.946	-8.196	-9.446
85		-2.822	-4.072	-5.322	-6.572	-7.822	-9.072
60		-2.444	-3.694	-4.944	-6.194	-7.444	-8.694
40		-2.003	-3.253	-4.503	-5.753	-7.003	-8.253
25		-1.493	-2.743	-3.993	-5.243	-6.493	-7.743
20		-1.251	-2.501	-3.751	-5.001	-6.251	-7.501
15		-0.939	-2.189	-3.439	-4.689	-5.939	-7.189
12		-0.696	-1.946	-3.196	-4.446	-5.696	-6.946
10		-0.498	-1.748	-2.998	-4.248	-5.498	-6.748
7		-0.111	-1.361	-2.611	-3.861	-5.111	-6.361
5		0.254	-0.996	-2.246	-3.496	-4.746	-5.996
4		0.497	-0.753	-2.003	-3.253	-4.503	-5.753
3		0.809	-0.441	-1.691	-2.941	-4.191	-5.441
2.5		1.007	-0.243	-1.493	-2.743	-3.993	-5.243
2		1.249	-0.001	-1.251	-2.501	-3.751	-5.001

Solar Mass	T_eff log g	15,000 K 2.00	16,000 K 5.00	16,000 K 4.50	16,000 K 4.00	16,000 K 3.50	16,000 K 3.00
120		-10.696	-3.477	-4.727	-5.977	-7.227	-8.477
85		-10.322	-3.102	-4.352	-5.602	-6.852	-8.102
60		-9.944	-2.724	-3.974	-5.224	-6.474	-7.724
40		-9.503	-2.284	-3.534	-4.784	-6.034	-7.284
25		-8.993	-1.773	-3.023	-4.273	-5.523	-6.773
20		-8.751	-1.531	-2.781	-4.031	-5.281	-6.531
15		-8.439	-1.219	-2.469	-3.719	-4.969	-6.219
12		-8.196	-0.977	-2.227	-3.477	-4.727	-5.977
10		-7.998	-0.779	-2.029	-3.279	-4.529	-5.779
7		-7.611	-0.391	-1.641	-2.891	-4.141	-5.391
5		-7.246	-0.026	-1.276	-2.526	-3.776	-5.026
4		-7.003	0.216	-1.034	-2.284	-3.534	-4.784
3		-6.691	0.529	-0.721	-1.971	-3.221	-4.471
2.5		-6.493	0.727	-0.523	-1.773	-3.023	-4.273
2		-6.251	0.969	-0.281	-1.531	-2.781	-4.031

Solar Mass	T_eff log g	16,000 K 2.50	16,000 K 2.00	17,000 K 5.00	17,000 K 4.50	17,000 K 4.00	17,000 K 3.50
120		-9.727	-10.977	-3.740	-4.990	-6.240	-7.490
85		-9.352	-10.602	-3.365	-4.615	-5.865	-7.115
60		-8.974	-10.224	-2.987	-4.237	-5.487	-6.737
40		-8.534	-9.784	-2.547	-3.797	-5.047	-6.297
25		-8.023	-9.273	-2.037	-3.287	-4.537	-5.787
20		-7.781	-9.031	-1.794	-3.044	-4.294	-5.544
15		-7.469	-8.719	-1.482	-2.732	-3.982	-5.232
12		-7.227	-8.477	-1.240	-2.490	-3.740	-4.990
10		-7.029	-8.279	-1.042	-2.292	-3.542	-4.792
7		-6.641	-7.891	-0.655	-1.905	-3.155	-4.405
5		-6.276	-7.526	-0.289	-1.539	-2.789	-4.039
4		-6.034	-7.284	-0.047	-1.297	-2.547	-3.797
3		-5.721	-6.971	0.265	-0.985	-2.235	-3.485
2.5		-5.523	-6.773	0.463	-0.787	-2.037	-3.287
2		-5.281	-6.531	0.706	-0.544	-1.794	-3.044

Solar Mass	T_eff log g	17,000 K 3.00	17,000 K 2.50	18,000 K 5.00	18,000 K 4.50	18,000 K 4.00	18,000 K 3.50
120		-8.740	-9.990	-3.988	-5.238	-6.488	-7.738
85		-8.365	-9.615	-3.614	-4.864	-6.114	-7.364
60		-7.987	-9.237	-3.236	-4.486	-5.736	-6.986
40		-7.547	-8.797	-2.795	-4.045	-5.295	-6.545
25		-7.037	-8.287	-2.285	-3.535	-4.785	-6.035
20		-6.794	-8.044	-2.043	-3.293	-4.543	-5.793
15		-6.482	-7.732	-1.730	-2.980	-4.230	-5.480
12		-6.240	-7.490	-1.488	-2.738	-3.988	-5.238
10		-6.042	-7.292	-1.290	-2.540	-3.790	-5.040
7		-5.655	-6.905	-0.903	-2.153	-3.403	-4.653
5		-5.289	-6.539	-0.538	-1.788	-3.038	-4.288
4		-5.047	-6.297	-0.295	-1.545	-2.795	-4.045
3		-4.735	-5.985	0.017	-1.233	-2.483	-3.733
2.5		-4.537	-5.787	0.215	-1.035	-2.285	-3.535
2		-4.294	-5.544	0.457	-0.793	-2.043	-3.293

Solar Mass	T_eff log g	18,000 K 3.00	18,000 K 2.50	19,000 K 5.00	19,000 K 4.50	19,000 K 4.00	19,000 K 3.50
120		-8.988	-10.238	-4.223	-5.473	-6.723	-7.973
85		-8.614	-9.864	-3.849	-5.099	-6.349	-7.599
60		-8.236	-9.486	-3.470	-4.720	-5.970	-7.220
40		-7.795	-9.045	-3.030	-4.280	-5.530	-6.780
25		-7.285	-8.535	-2.520	-3.770	-5.020	-6.270
20		-7.043	-8.293	-2.278	-3.528	-4.778	-6.028
15		-6.730	-7.980	-1.965	-3.215	-4.465	-5.715
12		-6.488	-7.738	-1.723	-2.973	-4.223	-5.473
10		-6.290	-7.540	-1.525	-2.775	-4.025	-5.275
7		-5.903	-7.153	-1.138	-2.388	-3.638	-4.888
5		-5.538	-6.788	-0.772	-2.022	-3.272	-4.522
4		-5.295	-6.545	-0.530	-1.780	-3.030	-4.280
3		-4.983	-6.233	-0.218	-1.468	-2.718	-3.968
2.5		-4.785	-6.035	-0.020	-1.270	-2.520	-3.770
2		-4.543	-5.793	0.222	-1.028	-2.278	-3.528

Solar Mass	T_eff log g	19,000 K 3.00	19,000 K 2.50	20,000 K 5.00	20,000 K 4.50	20,000 K 4.00	20,000 K 3.50
120		-9.223	-10.473	-4.446	-5.696	-6.946	-8.196
85		-8.849	-10.099	-4.071	-5.321	-6.571	-7.821
60		-8.470	-9.720	-3.693	-4.943	-6.193	-7.443
40		-8.030	-9.280	-3.253	-4.503	-5.753	-7.003
25		-7.520	-8.770	-2.743	-3.993	-5.243	-6.493
20		-7.278	-8.528	-2.500	-3.750	-5.000	-6.250
15		-6.965	-8.215	-2.188	-3.438	-4.688	-5.938
12		-6.723	-7.973	-1.946	-3.196	-4.446	-5.696
10		-6.525	-7.775	-1.748	-2.998	-4.248	-5.498
7		-6.138	-7.388	-1.360	-2.610	-3.860	-5.110
5		-5.772	-7.022	-0.995	-2.245	-3.495	-4.745
4		-5.530	-6.780	-0.753	-2.003	-3.253	-4.503
3		-5.218	-6.468	-0.441	-1.691	-2.941	-4.191
2.5		-5.020	-6.270	-0.243	-1.493	-2.743	-3.993
2		-4.778	-6.028	0.000	-1.250	-2.500	-3.750

Solar Mass	T_eff log g	20,000 K 3.00	21,000 K 5.00	21,000 K 4.50	21,000 K 4.00	21,000 K 3.50	21,000 K 3.00
120		-9.446	-4.658	-5.908	-7.158	-8.408	-9.658
85		-9.071	-4.283	-5.533	-6.783	-8.033	-9.283
60		-8.693	-3.905	-5.155	-6.405	-7.655	-8.905
40		-8.253	-3.465	-4.715	-5.965	-7.215	-8.465
25		-7.743	-2.954	-4.204	-5.454	-6.704	-7.954
20		-7.500	-2.712	-3.962	-5.212	-6.462	-7.712
15		-7.188	-2.400	-3.650	-4.900	-6.150	-7.400
12		-6.946	-2.158	-3.408	-4.658	-5.908	-7.158
10		-6.748	-1.960	-3.210	-4.460	-5.710	-6.960
7		-6.360	-1.572	-2.822	-4.072	-5.322	-6.572
5		-5.995	-1.207	-2.457	-3.707	-4.957	-6.207
4		-5.753	-0.965	-2.215	-3.465	-4.715	-5.965
3		-5.441	-0.652	-1.902	-3.152	-4.402	-5.652
2.5		-5.243	-0.454	-1.704	-2.954	-4.204	-5.454
2		-5.000	-0.212	-1.462	-2.712	-3.962	-5.212

Solar Mass	T_eff log g	22,000 K 5.00	22,000 K 4.50	22,000 K 4.00	22,000 K 3.50	22,000 K 3.00	23,000 K 5.00
120		-4.860	-6.110	-7.360	-8.610	-9.860	-5.053
85		-4.485	-5.735	-6.985	-8.235	-9.485	-4.678
60		-4.107	-5.357	-6.607	-7.857	-9.107	-4.300
40		-3.667	-4.917	-6.167	-7.417	-8.667	-3.860
25		-3.157	-4.407	-5.657	-6.907	-8.157	-3.350
20		-2.914	-4.164	-5.414	-6.664	-7.914	-3.107
15		-2.602	-3.852	-5.102	-6.352	-7.602	-2.795
12		-2.360	-3.610	-4.860	-6.110	-7.360	-2.553
10		-2.162	-3.412	-4.662	-5.912	-7.162	-2.355
7		-1.774	-3.024	-4.274	-5.524	-6.774	-1.967
5		-1.409	-2.659	-3.909	-5.159	-6.409	-1.602
4		-1.167	-2.417	-3.667	-4.917	-6.167	-1.360
3		-0.854	-2.104	-3.354	-4.604	-5.854	-1.048
2.5		-0.657	-1.907	-3.157	-4.407	-5.657	-0.850
2		-0.414	-1.664	-2.914	-4.164	-5.414	-0.607

Solar Mass	T_eff log g	23,000 K 4.50	23,000 K 4.00	23,000 K 3.50	23,000 K 3.00	24,000 K 5.00	24,000 K 4.50
120		-6.303	-7.553	-8.803	-10.053	-5.237	-6.487
85		-5.928	-7.178	-8.428	-9.678	-4.863	-6.113
60		-5.550	-6.800	-8.050	-9.300	-4.485	-5.735
40		-5.110	-6.360	-7.610	-8.860	-4.045	-5.295
25		-4.600	-5.850	-7.100	-8.350	-3.534	-4.784
20		-4.357	-5.607	-6.857	-8.107	-3.292	-4.542
15		-4.045	-5.295	-6.545	-7.795	-2.980	-4.230
12		-3.803	-5.053	-6.303	-7.553	-2.737	-3.987
10		-3.605	-4.855	-6.105	-7.355	-2.540	-3.790
7		-3.217	-4.467	-5.717	-6.967	-2.152	-3.402
5		-2.852	-4.102	-5.352	-6.602	-1.787	-3.037
4		-2.610	-3.860	-5.110	-6.360	-1.545	-2.795
3		-2.298	-3.548	-4.798	-6.048	-1.232	-2.482
2.5		-2.100	-3.350	-4.600	-5.850	-1.034	-2.284
2		-1.857	-3.107	-4.357	-5.607	-0.792	-2.042

Solar Mass	T_eff log g	24,000 K 4.00	24,000 K 3.50	24,000 K 3.00	25,000 K 5.00	25,000 K 4.50	25,000 K 4.00
120		-7.737	-8.987	-10.237	-5.415	-6.665	-7.915
85		-7.363	-8.613	-9.863	-5.040	-6.290	-7.540
60		-6.985	-8.235	-9.485	-4.662	-5.912	-7.162
40		-6.545	-7.795	-9.045	-4.222	-5.472	-6.722
25		-6.034	-7.284	-8.534	-3.712	-4.962	-6.212
20		-5.792	-7.042	-8.292	-3.469	-4.719	-5.969
15		-5.480	-6.730	-7.980	-3.157	-4.407	-5.657
12		-5.237	-6.487	-7.737	-2.915	-4.165	-5.415
10		-5.040	-6.290	-7.540	-2.717	-3.967	-5.217
7		-4.652	-5.902	-7.152	-2.330	-3.580	-4.830
5		-4.287	-5.537	-6.787	-1.964	-3.214	-4.464
4		-4.045	-5.295	-6.545	-1.722	-2.972	-4.222
3		-3.732	-4.982	-6.232	-1.410	-2.660	-3.910
2.5		-3.534	-4.784	-6.034	-1.212	-2.462	-3.712
2		-3.292	-4.542	-5.792	-0.969	-2.219	-3.469

Solar Mass	T_eff log g	25,000 K 3.50	25,000 K 3.00	26,000 K 5.00	26,000 K 4.50	26,000 K 4.00	26,000 K 3.50
120		-9.165	-10.415	-5.585	-6.835	-8.085	-9.335
85		-8.790	-10.040	-5.211	-6.461	-7.711	-8.961
60		-8.412	-9.662	-4.833	-6.083	-7.333	-8.583
40		-7.972	-9.222	-4.392	-5.642	-6.892	-8.142
25		-7.462	-8.712	-3.882	-5.132	-6.382	-7.632
20		-7.219	-8.469	-3.640	-4.890	-6.140	-7.390
15		-6.907	-8.157	-3.327	-4.577	-5.827	-7.077
12		-6.665	-7.915	-3.085	-4.335	-5.585	-6.835
10		-6.467	-7.717	-2.887	-4.137	-5.387	-6.637
7		-6.080	-7.330	-2.500	-3.750	-5.000	-6.250
5		-5.714	-6.964	-2.135	-3.385	-4.635	-5.885
4		-5.472	-6.722	-1.892	-3.142	-4.392	-5.642
3		-5.160	-6.410	-1.580	-2.830	-4.080	-5.330
2.5		-4.962	-6.212	-1.382	-2.632	-3.882	-5.132
2		-4.719	-5.969	-1.140	-2.390	-3.640	-4.890

Solar Mass	T_eff log g	26,000 K 3.00	27,000 K 5.00	27,000 K 4.50	27,000 K 4.00	27,000 K 3.50	28,000 K 5.00
120		-10.585	-5.749	-6.999	-8.249	-9.499	-5.907
85		-10.211	-5.375	-6.625	-7.875	-9.125	-5.533
60		-9.833	-4.996	-6.246	-7.496	-8.746	-5.154
40		-9.392	-4.556	-5.806	-7.056	-8.306	-4.714
25		-8.882	-4.046	-5.296	-6.546	-7.796	-4.204
20		-8.640	-3.804	-5.054	-6.304	-7.554	-3.962
15		-8.327	-3.491	-4.741	-5.991	-7.241	-3.649
12		-8.085	-3.249	-4.499	-5.749	-6.999	-3.407
10		-7.887	-3.051	-4.301	-5.551	-6.801	-3.209
7		-7.500	-2.664	-3.914	-5.164	-6.414	-2.822
5		-7.135	-2.298	-3.548	-4.798	-6.048	-2.456
4		-6.892	-2.056	-3.306	-4.556	-5.806	-2.214
3		-6.580	-1.744	-2.994	-4.244	-5.494	-1.902
2.5		-6.382	-1.546	-2.796	-4.046	-5.296	-1.704
2		-6.140	-1.304	-2.554	-3.804	-5.054	-1.462

Solar Mass	T_eff log g	28,000 K 4.50	28,000 K 4.00	28,000 K 3.50	29,000 K 5.00	29,000 K 4.50	29,000 K 4.00
120		-7.157	-8.407	-9.657	-6.059	-7.309	-8.559
85		-6.783	-8.033	-9.283	-5.685	-6.935	-8.185
60		-6.404	-7.654	-8.904	-5.307	-6.557	-7.807
40		-5.964	-7.214	-8.464	-4.867	-6.117	-7.367
25		-5.454	-6.704	-7.954	-4.356	-5.606	-6.856
20		-5.212	-6.462	-7.712	-4.114	-5.364	-6.614
15		-4.899	-6.149	-7.399	-3.802	-5.052	-6.302
12		-4.657	-5.907	-7.157	-3.559	-4.809	-6.059
10		-4.459	-5.709	-6.959	-3.361	-4.611	-5.861
7		-4.072	-5.322	-6.572	-2.974	-4.224	-5.474
5		-3.706	-4.956	-6.206	-2.609	-3.859	-5.109
4		-3.464	-4.714	-5.964	-2.367	-3.617	-4.867
3		-3.152	-4.402	-5.652	-2.054	-3.304	-4.554
2.5		-2.954	-4.204	-5.454	-1.856	-3.106	-4.356
2		-2.712	-3.962	-5.212	-1.614	-2.864	-4.114

Solar Mass	T_eff log g	29,000 K 3.50	30,000 K 5.00	30,000 K 4.50	30,000 K 4.00	30,000 K 3.50	31,000 K 5.00
120		-9.809	-6.207	-7.457	-8.707	-9.957	-6.349
85		-9.435	-5.832	-7.082	-8.332	-9.582	-5.975
60		-9.057	-5.454	-6.704	-7.954	-9.204	-5.596
40		-8.617	-5.014	-6.264	-7.514	-8.764	-5.156
25		-8.106	-4.503	-5.753	-7.003	-8.253	-4.646
20		-7.864	-4.261	-5.511	-6.761	-8.011	-4.404
15		-7.552	-3.949	-5.199	-6.449	-7.699	-4.091
12		-7.309	-3.707	-4.957	-6.207	-7.457	-3.849
10		-7.111	-3.509	-4.759	-6.009	-7.259	-3.651
7		-6.724	-3.121	-4.371	-5.621	-6.871	-3.264
5		-6.359	-2.756	-4.006	-5.256	-6.506	-2.898
4		-6.117	-2.514	-3.764	-5.014	-6.264	-2.656
3		-5.804	-2.201	-3.451	-4.701	-5.951	-2.344
2.5		-5.606	-2.003	-3.253	-4.503	-5.753	-2.146
2		-5.364	-1.761	-3.011	-4.261	-5.511	-1.904

Solar Mass	T_eff log g	31,000 K 4.50	31,000 K 4.00	31,000 K 3.50	32,000 K 5.00	32,000 K 4.50	32,000 K 4.00
120		-7.599	-8.849	-10.099	-6.487	-7.737	-8.987
85		-7.225	-8.475	-9.725	-6.112	-7.362	-8.612
60		-6.846	-8.096	-9.346	-5.734	-6.984	-8.234
40		-6.406	-7.656	-8.906	-5.294	-6.544	-7.794
25		-5.896	-7.146	-8.396	-4.784	-6.034	-7.284
20		-5.654	-6.904	-8.154	-4.542	-5.792	-7.042
15		-5.341	-6.591	-7.841	-4.229	-5.479	-6.729
12		-5.099	-6.349	-7.599	-3.987	-5.237	-6.487
10		-4.901	-6.151	-7.401	-3.789	-5.039	-6.289
7		-4.514	-5.764	-7.014	-3.402	-4.652	-5.902
5		-4.148	-5.398	-6.648	-3.036	-4.286	-5.536
4		-3.906	-5.156	-6.406	-2.794	-4.044	-5.294
3		-3.594	-4.844	-6.094	-2.482	-3.732	-4.982
2.5		-3.396	-4.646	-5.896	-2.284	-3.534	-4.784
2		-3.154	-4.404	-5.654	-2.042	-3.292	-4.542

Solar Mass	T_eff log g	33,000 K 5.00	33,000 K 4.50	33,000 K 4.00	34,000 K 5.00	34,000 K 4.50	34,000 K 4.00
120		-6.621	-7.871	-9.121	-6.750	-8.000	-9.250
85		-6.246	-7.496	-8.746	-6.376	-7.626	-8.876
60		-5.868	-7.118	-8.368	-5.998	-7.248	-8.498
40		-5.428	-6.678	-7.928	-5.557	-6.807	-8.057
25		-4.917	-6.167	-7.417	-5.047	-6.297	-7.547
20		-4.675	-5.925	-7.175	-4.805	-6.055	-7.305
15		-4.363	-5.613	-6.863	-4.492	-5.742	-6.992
12		-4.121	-5.371	-6.621	-4.250	-5.500	-6.750
10		-3.923	-5.173	-6.423	-4.052	-5.302	-6.552
7		-3.535	-4.785	-6.035	-3.665	-4.915	-6.165
5		-3.170	-4.420	-5.670	-3.300	-4.550	-5.800
4		-2.928	-4.178	-5.428	-3.057	-4.307	-5.557
3		-2.615	-3.865	-5.115	-2.745	-3.995	-5.245
2.5		-2.417	-3.667	-4.917	-2.547	-3.797	-5.047
2		-2.175	-3.425	-4.675	-2.305	-3.555	-4.805

Solar Mass	T_eff log g	35,000 K 5.00	35,000 K 4.50	35,000 K 4.00	36,000 K 5.00	36,000 K 4.50	36,000 K 4.00
120		-6.876	-8.126	-9.376	-6.998	-8.248	-9.498
85		-6.502	-7.752	-9.002	-6.624	-7.874	-9.124
60		-6.123	-7.373	-8.623	-6.246	-7.496	-8.746
40		-5.683	-6.933	-8.183	-5.806	-7.056	-8.306
25		-5.173	-6.423	-7.673	-5.295	-6.545	-7.795
20		-4.931	-6.181	-7.431	-5.053	-6.303	-7.553
15		-4.618	-5.868	-7.118	-4.741	-5.991	-7.241
12		-4.376	-5.626	-6.876	-4.498	-5.748	-6.998
10		-4.178	-5.428	-6.678	-4.300	-5.550	-6.800
7		-3.791	-5.041	-6.291	-3.913	-5.163	-6.413
5		-3.426	-4.676	-5.926	-3.548	-4.798	-6.048
4		-3.183	-4.433	-5.683	-3.306	-4.556	-5.806
3		-2.871	-4.121	-5.371	-2.993	-4.243	-5.493
2.5		-2.673	-3.923	-5.173	-2.795	-4.045	-5.295
2		-2.431	-3.681	-4.931	-2.553	-3.803	-5.053

Solar Mass	T_eff log g	37,000 K 5.00	37,000 K 4.50	37,000 K 4.00	38,000 K 5.00	38,000 K 4.50	38,000 K 4.00
120		-7.117	-8.367	-9.617	-7.233	-8.483	-9.733
85		-6.743	-7.993	-9.243	-6.859	-8.109	-9.359
60		-6.365	-7.615	-8.865	-6.481	-7.731	-8.981
40		-5.925	-7.175	-8.425	-6.040	-7.290	-8.540
25		-5.414	-6.664	-7.914	-5.530	-6.780	-8.030
20		-5.172	-6.422	-7.672	-5.288	-6.538	-7.788
15		-4.860	-6.110	-7.360	-4.975	-6.225	-7.475
12		-4.617	-5.867	-7.117	-4.733	-5.983	-7.233
10		-4.419	-5.669	-6.919	-4.535	-5.785	-7.035
7		-4.032	-5.282	-6.532	-4.148	-5.398	-6.648
5		-3.667	-4.917	-6.167	-3.783	-5.033	-6.283
4		-3.425	-4.675	-5.925	-3.540	-4.790	-6.040
3		-3.112	-4.362	-5.612	-3.228	-4.478	-5.728
2.5		-2.914	-4.164	-5.414	-3.030	-4.280	-5.530
2		-2.672	-3.922	-5.172	-2.788	-4.038	-5.288

Solar Mass	T_eff log g	39,000 K 5.00	39,000 K 4.50	39,000 K 4.00	40,000 K 5.00	40,000 K 4.50	40,000 K 4.00
120		-7.346	-8.596	-9.846	-7.456	-8.706	-9.956
85		-6.972	-8.222	-9.472	-7.082	-8.332	-9.582
60		-6.593	-7.843	-9.093	-6.703	-7.953	-9.203
40		-6.153	-7.403	-8.653	-6.263	-7.513	-8.763
25		-5.643	-6.893	-8.143	-5.753	-7.003	-8.253
20		-5.401	-6.651	-7.901	-5.511	-6.761	-8.011
15		-5.088	-6.338	-7.588	-5.198	-6.448	-7.698
12		-4.846	-6.096	-7.346	-4.956	-6.206	-7.456
10		-4.648	-5.898	-7.148	-4.758	-6.008	-7.258
7		-4.261	-5.511	-6.761	-4.371	-5.621	-6.871
5		-3.895	-5.145	-6.395	-4.005	-5.255	-6.505
4		-3.653	-4.903	-6.153	-3.763	-5.013	-6.263
3		-3.341	-4.591	-5.841	-3.451	-4.701	-5.951
2.5		-3.143	-4.393	-5.643	-3.253	-4.503	-5.753
2		-2.901	-4.151	-5.401	-3.011	-4.261	-5.511

Solar Mass	T_eff log g	41,000 K 5.00	41,000 K 4.50	42,000 K 5.00	42,000 K 4.50	43,000 K 5.00	43,000 K 4.50
120		-7.563	-8.813	-7.668	-8.918	-7.770	-9.020
85		-7.189	-8.439	-7.293	-8.543	-7.396	-8.646
60		-6.811	-8.061	-6.915	-8.165	-7.017	-8.267
40		-6.370	-7.620	-6.475	-7.725	-6.577	-7.827
25		-5.860	-7.110	-5.965	-7.215	-6.067	-7.317
20		-5.618	-6.868	-5.722	-6.972	-5.825	-7.075
15		-5.305	-6.555	-5.410	-6.660	-5.512	-6.762
12		-5.063	-6.313	-5.168	-6.418	-5.270	-6.520
10		-4.865	-6.115	-4.970	-6.220	-5.072	-6.322
7		-4.478	-5.728	-4.583	-5.833	-4.685	-5.935
5		-4.113	-5.363	-4.217	-5.467	-4.320	-5.570
4		-3.870	-5.120	-3.975	-5.225	-4.077	-5.327
3		-3.558	-4.808	-3.663	-4.913	-3.765	-5.015
2.5		-3.360	-4.610	-3.465	-4.715	-3.567	-4.817
2		-3.118	-4.368	-3.222	-4.472	-3.325	-4.575

Solar Mass	T_eff log g	44,000 K 5.00	44,000 K 4.50	45,000 K 5.00	45,000 K 4.50	46,000 K 5.00	46,000 K 4.50
120		-7.870	-9.120	-7.968	-9.218	-8.063	-9.313
85		-7.496	-8.745	-7.593	-8.843	-7.689	-8.939
60		-7.117	-8.367	-7.215	-8.465	-7.310	-8.560
40		-6.677	-7.927	-6.775	-8.025	-6.870	-8.120
25		-6.167	-7.417	-6.264	-7.514	-6.360	-7.610
20		-5.925	-7.175	-6.022	-7.272	-6.118	-7.368
15		-5.612	-6.862	-5.710	-6.960	-5.805	-7.055
12		-5.370	-6.620	-5.468	-6.718	-5.563	-6.813
10		-5.172	-6.422	-5.270	-6.520	-5.365	-6.615
7		-4.785	-6.035	-4.882	-6.132	-4.978	-6.228
5		-4.419	-5.669	-4.517	-5.767	-4.612	-5.862
4		-4.177	-5.427	-4.275	-5.525	-4.370	-5.620
3		-3.865	-5.115	-3.962	-5.212	-4.058	-5.308
2.5		-3.667	-4.917	-3.764	-5.014	-3.860	-5.110
2		-3.425	-4.675	-3.522	-4.772	-3.618	-4.868

Solar Mass	T_eff log g	47,000 K 5.00	47,000 K 4.50	48,000 K 5.00	48,000 K 4.50	49,000 K 5.00	49,000 K 4.50
120		-8.156	-9.406	-8.248	-9.498	-8.337	-9.587
85		-7.782	-9.032	-7.873	-9.123	-7.963	-9.213
60		-7.404	-8.654	-7.495	-8.745	-7.585	-8.835
40		-6.964	-8.214	-7.055	-8.305	-7.145	-8.395
25		-6.453	-7.703	-6.545	-7.795	-6.634	-7.884
20		-6.211	-7.461	-6.302	-7.552	-6.392	-7.642
15		-5.899	-7.149	-5.990	-7.240	-6.080	-7.330
12		-5.656	-6.906	-5.748	-6.998	-5.837	-7.087
10		-5.458	-6.708	-5.550	-6.800	-5.639	-6.889
7		-5.071	-6.321	-5.163	-6.413	-5.252	-6.502
5		-4.706	-5.956	-4.797	-6.047	-4.887	-6.137
4		-4.464	-5.714	-4.555	-5.805	-4.645	-5.895
3		-4.151	-5.401	-4.243	-5.493	-4.332	-5.582
2.5		-3.953	-5.203	-4.045	-5.295	-4.134	-5.384
2		-3.711	-4.961	-3.802	-5.052	-3.892	-5.142

Solar Mass	T_eff log g	50,000 K 5.00	50,000 K 4.50
120		-8.425	-9.675
85		-8.051	-9.301
60		-7.673	-8.923
40		-7.232	-8.482
25		-6.722	-7.972
20		-6.480	-7.730
15		-6.167	-7.417
12		-5.925	-7.175
10		-5.727	-6.977
7		-5.340	-6.590
5		-4.975	-6.225
4		-4.732	-5.982
3		-4.420	-5.670
2.5		-4.222	-5.472
2		-3.980	-5.230

APPENDIX B

IUE LOG IMAGE NUMBERS WITH STELLAR NAMES AND SPECTRAL TYPE

IUE Image Number	IUE Log	Sanduleak	Bright Star	Radcliffe	Henize	Sp. Type	Sp. Type	
LWP/LWR	SWP	Name	Catalog	Catalog	Number	Number	Simbad	
LWR 13453	17173	268654	SK -69 7	HD 268654	RMC 52	-	B8Iab	B9Ia
LWP 15648	36388	SK-69 08	SK -69 08	HD 268657	-	-	B5Ia	B5Ib
LWR 4170	4827	268605	SK -67 5	HD 268605	RMC 53	-	B0Ia	B0
LWP 10434	30620	268718	SK -69 16	HD 268718	RMC 55	S 69	B9Iabe..	B9Iab
LWP 8788	28797	SK-66 1	SK -66 1	HD 268623	RMC 56	-	B2Ia	B3Ia
LWP 5943	25897	SK-69 19	SK -69 19	-	-	-	B0.5	B0Ia
LWP 10832	31043	S-68 5	SK -68 5	-	-	-	Be	O6Iab
LWP 5977	25937	SK-66 5	SK -66 5	HD 268653	RMC 57	-	B3Iab..	B3Ib
LWP 15674	36415	SK-68 08	SK -68 08	HD 268729	RMC 58	-	B5Iab..	B4Ib
LWP 17962	38848	SK-67 15	SK -67 15	HD 268690	-	-	B7Ia	B7Ib
LWP 15649	36389	SK-69 32	SK -69 32	HD 268788	-	-	B3Iab	B3Ib
LWR 17292	22496	SK-66 27	SK -66 27	-	-	-	B2	B2Ia
LWP 8750	28763	SK-69 43	SK -69 43	HD 268809	RMC 65	-	B1Ia	B0Ia
LWP 17961	38847	SK-66 36	SK -66 36	HD 268726	-	-	B1Iab	B1
LWP 5944	25898	SK-69 45	SK -69 45	-	-	-	B1	B0Ia
LWP 5945	25899	SK-68 11	SK -68 11	-	-	-	B1	B0Ib
LWP 10451	30656	268804	SK -68 14	HD 268804	-	-	B2Iab	B2Iab
LWP 16024	36764	SK-69 52	SK -69 52	HD 268867	-	-	B2Ia	B2Ib
LWP 15904	36666	SK-65 04	SK -65 4	HD 270918	-	-	O...	B0I
LWP 18087	39065	SK-67 27	SK -67 27	-	-	-	-	B6Ib
LWP 8775	28784	SK-67 28	SK -67 28	-	-	-	B1	B0Ia
LWP 5969	25932	SK-65 15	SK -65 15	-	-	-	O...	B1Ib
LWP 15682	36425	SK-65 16	SK -65 16	-	-	-	O...	B2Ib
LWP 15650	36390	SK-70 30	SK -70 30	-	-	-	-	B5Ib
LWP 15905	36667	SK-65 19	SK -65 19	HD 270948	-	-	O...	B0I
LWP 18198	39155	SK-68 23	SK -68 23	-	-	-	-	B0
LWP 5978	25938	SK-65 20	SK -65 20	HD 270949	RMC 70	-	B3Iab...	B3Ib
LWP 5968	25931	SK-65 21	SK -65 21	-	-	-	B2II	B0Ia
LWP 15675	36416	SK-67 36	SK -67 36	-	-	-	-	B2Ib
LWR 17302	22519	SK-68 26	SK -68 26	-	-	-	B8:Iab:	B0Ia
LWP 15742	36541	SK-70 44	SK -70 44	HD 268984	-	-	B2.5Ia	B3Ib
LWP 17960	38846	SK-66 50	SK -66 50	HD 268907	RMC 73	-	B8Ia	B7Ib
LWP 15673	36414	SK-70 48	SK -70 48	HD 269018	-	-	B3Ia	B2Ib
LWP 18545	39428	SK-67 39	SK -67 39	-	-	-	B6Iab:	B6Ib
LWP 8753	28765	SK-70 50	SK -70 50	HD 269009	-	-	B5	B5Ia
LWP 15652	36392	SK-70 51	SK -70 51	HD 269013	-	-	B3Iab:	B3Ib
LWP 18546	39429	SK-67239	SK -67 239	HD 270003	-	-	B8Iab:	B6Ib
LWR 17290	22493	SK-67 43	SK -67 43	-	-	-	B2	B2Ia
LWP 18168	39132	SK-68 39	SK -68 39	-	-	-	B2.5Ia	B1Ib
LWP 5941	25895	SK-70 58	SK -70 58	-	-	-	B0.5	B0Ib
LWR 15477	19452	SK-70 60	SK -70 60	-	-	-	O4V	O5
LWP 9939	30108	NS 29-65	SK -65 29	-	-	-	O8V	O8V

IUE Image Number LWP/LWR	IUE Log SWP	IUE Log Name	Sanduleak Catalog	Bright Star Catalog	Radcliffe Number	Henize Number	Sp. Type Simbad	Sp. Type IUE Log
LWR 15594	19561	SK-68 41	SK -68 41	-	-	-	B0.5Ia	B0Ia
LWP 9940	30109	NS 69-70	SK -70 69	-	-	-	O4V	O4V
LWP 10462	30673	S-68 42	SK -68 42	-	-	-	-	B0Iab
LWP 10523	30745	SK-68 45	SK -68 45	-	-	-	B0	B0Ia
LWP 5946	25900	SK-68 46	SK -68 46	-	-	-	B0	B0Ib
LWP 8740	28758	SK-70 78	SK -70 78	HD 269074	-	-	B1	B1Ia
LWR 3632	4095	269074	SK -70 78	HD 269074	-	-	B1	B1Ib
LWP 5942	25896	SK-70 79	SK -70 79	-	-	-	O...	B0Ib
LWP 17912	38795	SK-70 80	SK -70 80	-	-	-	B8Iab	B0Ib
LWR 15476	19451	SK-67 51	SK -67 51	-	-	-	O6.5III	O6
LWP 5966	25929	SK-68 58	SK -68 58	HD 269101	RMC 79	-	B5Iab...	B5Ib
LWP 15954	36699	SK-68 59	SK -68 59	HD 269116	-	-	B0.7Ia	B1Ib
LWP 18169	39133	SK-68 62	SK -68 62	HD 269117	-	-	B6Iab:	B6Ib
LWP 15906	36668	SK-67 58	SK -67 58	HD 269145	-	-	G0Ia	B3Ib
LWR 8074	9313	Dachs 1-9	-	-	-	-	B0.5Ib	B0Ia
LWR 11632	15115	S 89	SK -69 77	HD 269217	RMC 82	S 89	-	O9
LWR 10155	13507	LMC S89	SK -69 77	HD 269217	RMC 82	S 89	-	O9
LWP 15678	36421	SK-67 66	SK -67 66	HD 269189	-	-	B6Ia	B5Ib
LWR 15586	19551	SK-69 89	SK -69 89	HD 269311	-	-	B2.5Ia	B1Ia
LWP 15955	36700	SK-70 85	SK -70 85	HD 269314	-	-	-	B0Ib
LWR 15587	19552	SK-69 91	SK -69 91	HD 269327	-	-	-	B0Ia
LWP 10410	30601	269321	SK -69 92	HD 269321	RMC 85	-	-	B5Iab
LWR 11629	15112	S 96	SK -69 94	HD 35343	RMC 88	S 96	A0e...	O9
LWP 15688	36431	SK-65 40	SK -65 40	HD 271163	-	-	B3Ia	B3Ib
LWP 15704	36449	SK-69100	SK -69 100	HD 269351	-	-	G2Ia	B5Ib
LWR 4174	4831	269357	SK -69 104	HD 269357	-	-	09.5Iab:	O9
LWR 17296	22509	SK-67 78	SK -67 78	HD 269371	-	-	B3Ia	B3Ia
LWP 15705	36450	SK-69110	SK -69 110	HD 269399	-	-	B3Ia	B3Ib
LWP 16036	36773	SK-69111	SK -69 111	-	-	-	-	B2Ib
LWR 8075	9314	R 93	SK -65 51	-	RMC 93	-	B0	B0Ia
LWP 15680	36423	SK-67 81	SK -67 81	HD 269400	-	-	B5Ia	B5Ib
LWP 15679	36422	SK-67 84	SK -67 84	HD 269412	-	-	B	B2
LWP 5940	25894	SK-6872A	SK -68 72a	-	-	-	F9	B0Ib
LWR 15595	19562	SK-67 90	SK -67 90	HD 269440	-	-	F6III	B1Ia
LWP 18166	39130	SK-66 78	SK -66 78	-	-	-	B1Ia	B1
LWP 16026	36766	SK-71 23	SK -71 23	HD 269475	RMC 100	-	B3Iab...	B5Ib
LWP 5947	25901	SK-68 75	SK -68 75	HD 269463	-	-	B0.5	B0Ia
LWP 16020	36760	SK-66 79	SK -66 79	HD 269452	-	-	B3Iab:	B3Ib
LWP 5939	25893	SK-66 86	SK -66 86	-	-	-	B0.5	B0Ib
LWP 18165	39129	SK-66 88	SK -66 88	-	-	-	-	B2
LWP 5980	25940	SK-67108	SK -66 108	-	-	-	B0	B0Ia
LWP 13584	33877	LH58:14	-	-	-	-	-	O6V

IUE Image Number	IUE Log	Sanduleak	Bright Star	Radcliffe	Henize	Sp. Type	Sp. Type
LWP/LWR	SWP	Name	Catalog	Catalog	Number	Number	Simbad IUE Log
LWP 13425	33754	LH58:52A	-	-	-	-	O8II
LWP 13583	33876	LH58:10	-	-	-	-	O8III
LWP 13426	33755	LH58:30	-	-	-	-	O7V
LWP 15743	36542	SK-71 30	SK -71 30	HD 269547	RMC 101	-	B3Ia B5Ib
LWP 13427	33757	LH58:10A	-	-	-	-	O3V
LWR 15596	19563	SK-67112	SK -67 112	HD 269545	-	-	B1Ia B1Ia
LWP 15709	36454	SK-67116	SK -67 116	HD 269559	-	-	B3Ia B3Ib
LWP 10438	30634	-67 117A	SK-67 117a	-	-	-	B0Iab
LWP 5955	25911	SK-67117	SK -67 117	-	-	-	O9 B0Ib
LWP 15707	36452	SK-69139	SK -69 139	-	-	-	B3Iab: B3Ib
LWR 15475	19450	SK-66100	SK -66 100	-	-	-	O6III O6
LWP 15692	36435	SK-67122	SK -67 122	HD 269577	-	-	B6Ia B5Ib
LWP 16021	36761	SK-68 87	SK -68 87	-	-	-	B2Ib
LWP 15697	36441	SK-69143	SK -69 143	-	-	-	A4Ia B5Ib
LWP 15691	36434	SK-67126	SK -67 126	HD 269593	-	-	B5Ia B5Ib
LWP 5957	25913	SK-65 63	SK -65 63	HD 271294	-	-	- B0Ib
LWP 8785	28796	SK-68 92	SK -68 92	-	-	-	B0.5Iab: B2Ia
LWP 15695	36439	SK-69149	SK -69 149	-	-	-	B6Iab: B5Ib
LWP 8749	28762	SK-67130	SK -67 130	HD 269606	-	-	B7Ia B8Ia
LWP 8751	28764	SK-66106	SK -66 106	-	-	-	B1.5Ia B1Ia
LWP 15681	36424	SK-66107	SK -66 107	-	-	-	- B5Ib
LWR 14199	17988	269619	SK -68 100	HD 269619	-	-	A0Ia B9Ia
LWP 15689	36432	SK-67137	SK -67 137	HD 269629	-	-	B6Iab: B4Ib
LWP 15690	36433	SK-67138	SK -67 138	-	-	-	B8Iab: B5Ib
LWP 10469	30682	S-69 160	SK -69 160	-	-	-	B1.5: O9Iab
LWP 15696	36440	SK-69162	SK -69 162	-	-	-	B1 B2Ib
LWP 15754	36555	SK-66118	SK -66 118	-	-	-	B2Iab B2Ib
LWP 18566	39445	-67153	SK -67 153	-	-	-	- B7Ib
LWP 15693	36437	SK-69172	SK -69 172	-	-	-	- B3Ib
LWR 15579	19541	SK-67168	SK -67 168	HD 269702	-	-	O8Ia... B0Ia
LWP 5954	25910	SK-67167	SK -67 167	-	-	-	O4 B0Ib
LWP 15703	36448	SK-69177	SK -69 177	-	-	-	- B4Ib
LWP 18159	39123	SK-67174	SK -67 174	HD 269714	-	-	O9 O9II
LWP 15694	36438	SK-69179	SK -69 179	HD 269705	-	-	B2 B2Ib
LWP 10411	30602	S-67 177	SK -67 177	-	-	-	B8Iab: B1Iab
LWP 18059	39038	SK-69181	SK -69 181	-	-	-	- B1
LWP 10453	30658	S-67 179	SK -67 179	-	-	-	- B1Iab
LWP 15952	36697	SK-68121	SK -68 121	-	-	-	B2 B2
LWR 16736	20929	SK-67191	SK -67 191	-	-	-	O8V O7V
LWP 15752	36553	SK-66143	SK -66 143	HD 269761	-	-	B5Iab: B5Ib
LWP 10458	30662	S-67 197	SK -67 197	-	-	-	B6Iab: B6Iab
LWP 5956	25912	SK-66152	SK -66 152	-	-	-	O8 B0Ib

IUE Image Number LWP/LWR SWP	IUE Name	Sanduleak Catalog	Bright Star Catalog	Radcliffe Number	Henize Number	Sp. Type Simbad	Sp. Type IUE Log
LWP 18078	39055	SK-69193	SK -69 193	HD 269769	-	-	B1
LWP 5979	25939	SK-67206	SK -67 206	-	-	B1Ia	B0Ia
LWP 16022	36762	SK-69197	SK -69 197	HD 269784	-	O	B2Ib
LWR 17286	22482	SK-69199	SK -69 199	-	-	-	B1Ia
LWP 18199	39156	SK-67214	SK -67 214	HD 269833	-	B8Iab	B6Ib
LWP 12745	32988	SK-69203	SK -69 203	-	-	B0.7Ia	B0Ib
LWP 18079	39056	SK-69205	SK -69 205	-	-	-	B1
LWP 18161	39125	SK-67217	SK -67 217	HD 269844	-	B1.5Iab	B1
LWR 15585	19550	SK-68126	SK -68 126	-	-	-	B2Ia
LWP 15751	36552	SK-69206	SK -69 206	-	-	B2	B2Ib
LWP 16023	36763	SK-66166	SK -66 166	HD 269863	-	B2Ia	B2Ib
LWP 18162	39126	SK-67222	SK -67 222	HD 269854	-	B5Ia	B7Ib
LWP 15755	36556	SK-67220	SK -67 220	HD 269845	RMC 125	B3Iab...	B2Ib
LWR 17287	22483	SK-68129	SK -68 129	-	-	-	B1Ia
LWP 10452	30657	269846	SK -69 215	HD 269846	-	-	B0Iab
LWP 8741	28759	SK-66169	SK -66 169	HD 269889	-	09.7Ia	O9Ia
LWR 16729	20915	SK-66172	SK -66 172	-	-	O5V	O9V
LWP 19013	39834	SK-66178	SK -66 178	-	-	-	B1
LWR 4261	4932	SK-67228	SK -67 228	HD 269900	-	B1Ia	B1Ib
LWP 15756	36557	SK-69236	SK -69 236	-	-	-	B2Ib
LWP 18080	39057	SK-69237	SK -69 237	-	-	B1Ia	B1
LWR 11590	15050	R 133	-	-	RMC 133	O8	O8
LWP 18086	39064	SK-69252	SK -69 252	-	-	-	B0
LWP 18085	39063	SK-69261	SK -69 261	-	-	B0.5	B0
LWP 18534	39413	SK-69264	SK -69 264	-	-	B6Iab:	B7Ib
LWR 15593	19560	SK-69265	SK -69 265	-	-	-	B3Ia
LWR 13467	17184	269997	SK -69 270	HD 269997	-	B3Ia	B3Ia
LWP 15953	36698	SK-69271	SK -69 271	-	-	-	B2Ib
LWP 5967	25930	SK-69276	SK -69 276	-	-	B0Iab	B0Ib
LWR 15581	19543	SK-69282	SK -69 282	HD 270019	-	B1	B1Ia
LWP 18170	39134	SK-69290	SK -69 290	-	-	B...	B0
LWR 15580	19542	SK-68155	SK -68 155	-	-	-	B0Ia
LWR 17288	22484	SK-71 52	SK -71 52	-	-	-	B0Ib
LWP 8784	28795	SK-67255	SK -67 255	HD 270094	-	B4	B7Ia
LWR 15582	19544	SK-67256	SK -67 256	-	-	B1.5Ia	B1Ia
LWP 18535	39414	SK-67258	SK -67 258	HD 270105	-	B6Iab:	B7Ib
LWP 11212	31340	SK-70115	SK -70 115	HD 270145	-	O6.5III	O6III
LWP 13585	33878	LH117:13	-	-	-	-	O4V
LWP 13272	33575	LH117:43	-	-	-	-	O6V
LWP 13270	33573	LH117:11	-	-	-	-	O3III
LWP 17913	38796	SK-68171	SK -68 171	HD 270220	-	B0.7Ia	B1Ib

VITA

Kenneth Thomas Taylor was born in Keesler Air Force Base, Biloxi, Mississippi, on February 12, 1959. He attended Biloxi High School and graduated in 1977. He was awarded a Bachelor of Science degree in physics from Tulane University in May, 1984, and is presently a candidate for the degree of Master of Science in the Department of Physics and Astronomy at Louisiana State University.